Supramolecular Ru nanocatalyst, based on a β-cyclodextrin copolymer with epichlorohydrin, in the hydrogenation of unsaturated compounds*

A. L. Maximov, A. V. Zolotukhina,★ and E. R. Naranov

A. V. Topchiev Institute of Petrochemical Synthesis, Russian Academy of Sciences, 29 Leninsky prosp., 119991 Moscow, Russian Federation.
E-mail: anisole@yandex.ru

A water-soluble catalyst based on ruthenium(0) nanoparticles stabilized with copolymer based on β-cyclodextrin and epichlorohydrin was synthesized and characterized by transmission electron microscopy, small-angle X-ray scattering, and X-ray photoelectron spectroscopy. The catalyst obtained was tested in the hydrogenation of various substrates, such as aromatic and unsaturated compounds, phenols, levulinic acid and its esters for the first time. The catalyst activity was found to depend considerably on the substrate polarity and size. The size of the non-polar moiety of the substrate was that specifying its propensity to form inclusion complexes with β-cyclodextrin moieties of the carrier. For aromatic compounds, the latter acted as a protecting group.

Key words: hydrogenation, Ru nanoparticles, cyclodextrins, polymeric catalyst.

In recent years, nanostructured systems based on metal nanoparticles,[1] oxides,[2] sulfides,[3] and phosphides[4] became particularly important for catalysis due to their small sizes, high dispersity, and, as a result, high total specific surface area, which provides a high reaction rate and turnover frequency. To stabilize these systems, both ordered carriers based on carbon materials,[5] silica, zeolites and natural clays,[6] alumina, titania, and ceria,[7] hybrid organic-inorganic materials,[8] and various organic ligands with donor atoms (O, N, P, and S)[9,10] are widely used. Of particular interest are polymeric[11,12] and macrocyclic ligands[13,14] capable of forming supramolecular assemblies with a substrate due to a combination of electrostatic, van der Waals, hydrophobic, π—π-interactions and hydrogen bonds.[11—14] These supramolecular systems affect the substrate orientation relative to the catalytically active site, and thus can not only considerably increase its conversion rate, but also provide unusual substrate selectivity and regiospecificity of the reaction.[11—14]

An important feature of macrocyclic receptor molecules, such as crown ethers, cryptands, calix- and pillararenes, cucurbiturils and cyclodextrins, is their ability for molecular recognition, which manifests itself in the "capture" of ions or organic molecules of the appropriate size by the macrocycle due to electrostatic or hydrophobic interactions with the formation of guest—host complexes.[13,14] Among these molecules, it is worth to note cyclodextrins, which are the natural cyclic oligomers consisting of α-D-glucopyranose fragments linked by α-(1→4)-glycosidic bonds.[15] The most common are α-, β-, and γ-cyclodextrins (CDs), which consist of six, seven, and eight glucopyranose fragments of 5.7, 7.8, and 9.5 Å in size, respectively.[16]

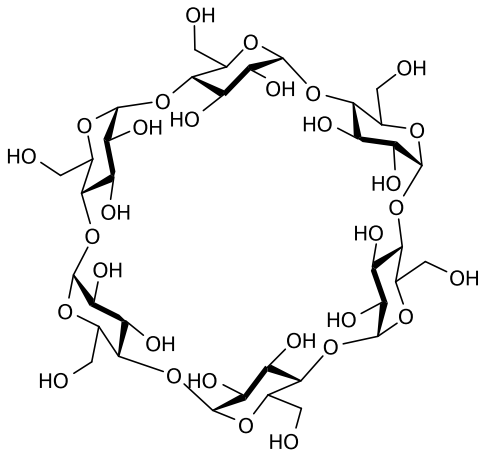

α-CD

* Dedicated to Academician of the Russian Academy of Sciences I. P. Beletskaya on the occasion of her anniversary.

Published in Russian in *Izvestiya Akademii Nauk. Seriya Khimicheskaya,* Vol. 72, No. 4, pp. 853—872, April, 2023.
1066-5285/23/7204-0853

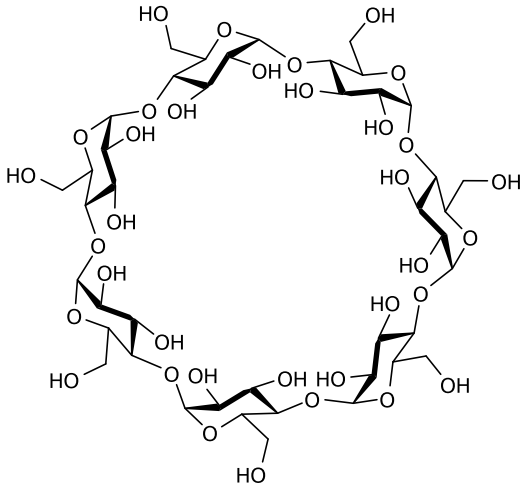

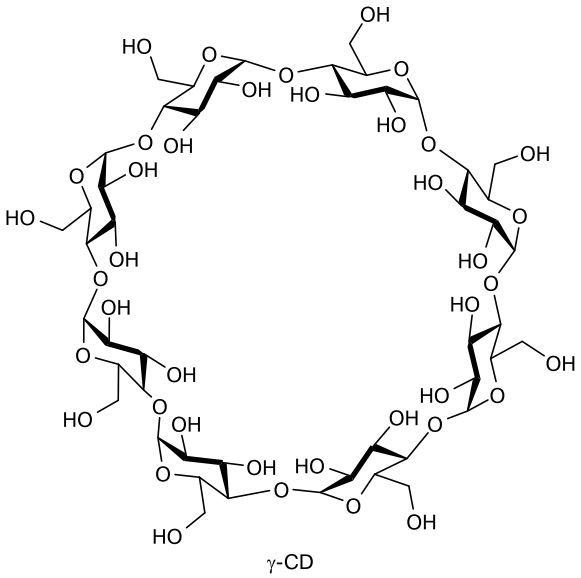

The combination of a hydrophilic surface and a hydrophobic cavity in the structure of cyclodextrins (Fig. 1) ensures their ability to form guest—host-type inclusion complexes in polar media with organic molecules of appropriate sizes and their transfer into the aqueous phase.[16,17] Modification of cyclodextrin hydroxyl groups makes it possible to considerably change both the binding constants of the guest molecules and their orientation in the cyclodextrin cavity.[17,18]

The use of cyclodextrins for the stabilization of metal nanoparticles (NPs) makes it possible to obtain highly selective catalysts that ensure a high conversion of the substrate, including under conditions of two-phase reactions. Thus, the use of catalysts based

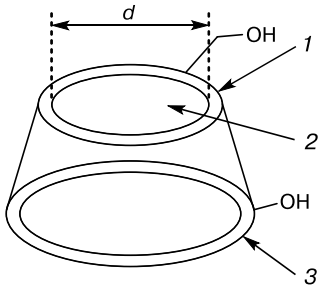

Fig. 1. Schematic representation of a β-cyclodextrin (β-CD) molecule:[16] *1*, upper rim (primary hydroxyl groups), *2*, hydrophobic cavity, *3*, lower rim (secondary hydroxyl groups); $d = 7.8$ Å.

on ruthenium NPs stabilized with methylated cyclodextrins in the hydrogenation of styrene or allylbenzene in an aqueous medium made it possible to control the selectivity of the reaction by varying the size and methylation degree of cyclodextrin.[19] A catalyst based on rhodium NPs stabilized by β-CD cross-linked with an alt-copolymer of maleic anhydride and methyl vinyl ether provided exhaustive hydrogenation of alkenes and aromatic compounds under two-phase conditions[20] and a 100% selectivity for cyclohexanone in phenol hydrogenation for reactions carried out not only in an ionic liquid medium, but also in water even under the excess hydrogen pressure and a considerable reaction time.[21] Ruthenium nanoparticles, stabilized with β-CD cross-linked with polyethylene glycol (PEG) diglycidyl ether, proved to be efficient and selective catalysts for the hydrogenation of levulinic acid (LA) to γ-valerolactone (γ-VL) in an aqueous medium compared to the traditional Ru/C catalyst.[22]

Water-soluble polymers based on cyclodextrins cross-linked with epichlorohydrin are the simplest and most promising materials for the stabilization of metal NPs in an aqueous medium. As a rule, they are a mixture of branched polyglycidyl oligomers containing one or several cyclodextrin moieties, the composition and properties of which are considerably dependent on the synthesis conditions.[23—25] In this work, we propose to use a new catalytic system based on ruthenium NPs dispersed in an aqueous medium and stabilized with a low molecular weight polymer of this type for hydrogenation. Attaching the β-CD moieties to the stabilizing surface layer of the NPs makes it possible to achieve high efficiency and, in some cases, unusual substrate selectivity in the hydrogenation of aromatic and unsaturated compounds, phenols, LA and its esters.

Experimental

Reagents. The following chemicals were used for the synthesis of catalytic systems: β-cyclodextrin (β-CD) $(\alpha\text{-}C_6H_{10}O_5)_7 \cdot x\ H_2O$ (x = 0—1) (99%, Acros Organics, Hungary), epichlorohydrin CH_2OCHCH_2Cl (99%, Aldrich, Germany), NaOH (reagent grade, Komponent-Reaktiv, Russia), concentrated HCl (reagent grade, Komponent-Reaktiv, Russia), $RuCl_3 \cdot xH_2O$ (x = 0—3) (pure grade, 47.80% content of Ru, Aurat JSC, Russia); sodium borohydride $NaBH_4$ (⩾98%, Aldrich, USA). The following reagents were used as substrates and standards: benzene (analytical grade, IREA 2000, Russia); cyclohexane (pure grade, Reakhim, Russia); cyclohexene (99%, Aldrich, Germany); biphenyl (99.5%, Aldrich, Germany); *trans*-stilbene *trans*-$C_6H_5{-}CH_2{=}CH_2{-}C_6H_5$ (99%, Aldrich, Germany); phenol (pure grade, Reakhim, Russia); cyclohexanol (Ferak, Germany); cyclohexanone (Jenapharm Apolda, pro analysi, Germany); 2-cyclohexenone (⩾95%, Aldrich); 4-*tert*-butylphenol (97%, Lancaster, UK); *tert*-butylbenzene (pure grade, Reakhim, Russia); levulinic acid (98%, Aldrich, Germany). Levulinic acid esters (methyl levulinate, ethyl levulinate, and butyl levulinate) were obtained according to the standard procedure by esterification of levulinic acid with the corresponding alcohols in an acid medium.[26] Solvents, namely, acetone (reagent grade, Komponent-Reaktiv, Russia), diethyl ether $(C_2H_5)_2O$ (analytical grade, Ekos-1, Russia), C_2H_5OH (reagent grade, Ekos-1, Russia), propan-2-ol (reagent grade, Komponent-Reaktiv, Russia), toluene (analytical grade, Ekos-1, Russia), were used without preliminary purification.

Methods and devices. NMR spectra were recorded at 25 °C on a Bruker AVANCE III HD spectrometer using a PI HR-BBO400S1-BBF/H/D-5.0-Z SP probe (400.13 (^{1}H) and 100.62 (^{13}C) MHz) in a stationary magnetic field of 9.389 T. The solvents were D_2O and DMSO-d_6. ^{1}H NMR spectra were recorded with presaturation of the HOD signal, ^{13}C NMR spectra were recorded with broadband decoupling from protons (relaxation delay D1 = 2 s, number of scans NS = 8000). Chemical shifts of the ^{1}H and ^{13}C signals are given relative to the internal standards, tetramethylsilane (TMS, δ 0.00) or 3-(trimethylsilyl)-propanesulfonic acid (DSS, δ 0.015). Mass spectrometry with matrix-assisted laser desorption/ionization (MS-MALDI) was performed on a Bruker Autoflex Speed mass spectrometer equipped with a solid-state laser (λ = 355 nm) and a time-of-flight detector in the linear positive ion detection mode, mass scan range m/z 200—6000. An aqueous solution of 3-aminoquinoline (30 mg mL^{-1}) was used as a matrix. Before carrying out measurements, aqueous solutions of the matrix and analytes (2 mg mL^{-1}) were mixed, deposited on a steel target, and dried. The data were processed using the Bruker Compass 1.4 software package. IR spectra of the carrier and catalyst samples were recorded on a Nicolet IR 2000 Fourier-transform IR spectrometer (Thermo Scientific) using a Multi-reflection HATR attachment containing a 45° ZnSe crystal to provide multiple frustrations of total internal reflection in the wavelength range 4000—500 cm^{-1} with a resolution of 4 cm^{-1}. The bond energies and oxidation states of the elements on the surface of the catalyst sample were determined by X-ray photoelectron spectroscopy (XPS) on a PREVAC EA15 electron spectrometer. The spectra of the samples were recorded using monochromatic radiation of an aluminum anode Al-Kα ($h\nu$ = 1486.6 eV) with a tube voltage of 12 kV, an emission current of 20 mA, and a power of 150 W. The pressure in the spectrometer chamber during analysis did not exceed $3.75 \cdot 10^{-9}$ Torr. The preliminary calibration of the energy scale of the spectrometer corresponded to the following values of the peaks of standard samples Ag $3d_{5/2}$ (368.3 eV) and Au $4f_{7/2}$ (84.0 eV) of silver and gold foil, respectively. The spectra were calibrated taking into account the surface charge using the C 1s (284.8 eV) and O 1s (532.5 eV) lines selected as internal standards. The catalyst sample morphology and particle size distribution were studied by transmission electron microscopy (TEM) on a JEM-2100 JEOL electron microscope with an electron tube voltage of 100 kV. The sample was dispersed in ethanol before being deposited on the substrate. The obtained microphotographs were processed using the Image J program (https://imagej.net/ij/features.html). Small-angle X-ray scattering (SAXS) was carried out on a BioMUR instrument (Kurchatov Synchrotron Radiation Source) with an incident radiation energy of 8.58 keV (λ = 1.445 Å).[27] The data were recorded on a Dectris Pilatus 1 M detector over 60 s. The instrument was preliminarily calibrated using silver behenate ($C_{21}H_{43}COOAg$). To obtain an image, the sample was placed between two layers of Kapton tape. The range of scattering vectors s was 0.1—5.5 nm^{-1} ($s = 4\pi\sin(\theta)/\lambda$, 2θ is the scattering angle). Four images were recorded in total and then radially averaged using the Fit2D Software, followed by normalization to the transmitted beam intensity;[28] the scattering signal of the Kapton tape was subtracted. The pair distribution function $P(r)$ was obtained using the Primus ATSAS software in the range of scattering vectors of 0.15—2.2 nm^{-1} for the model of polydisperse spheres.[29] The quantitative content of ruthenium in the sample was determined by inductively coupled plasma atomic emission spectroscopy (ICP-AES) on an IRIS Intrepid II XPL device (Thermo Electron Corp.) in the radial and axial measurement modes at wavelengths of 310 and 95.5 nm. Before analysis, the samples were preliminarily treated with concentrated H_2SO_4 (reagent grade, Khimmed) and then dissolved in aqua regia. Qualitative and quantitative analysis of hydrogenation products was carried out by gas-liquid chromatography (GLC) on a ChromPack CP9001 chromatograph equipped with a flame ionization

detector and a capillary column (30 m×0.2 mm) with SE-30 bonded phase, using known standards for identification. Product identification was additionally monitored using a Leco Pegasus® GC-HRT 4D time-of-flight chromatomass spectrometer equipped with a flame ionization detector. The structures of components were established by mass spectra using the data of the NIST v.2.3 library dated 04.05.2017.

Synthesis of water-soluble cyclodextrin-containing polymer β-CD-Glycd was carried out according to the procedure.[23] β-Cyclodextrin (1.150 g, 1 mmol), NaOH (1 g, ~25 mmol), and distilled water (125 mL) were mixed in a 150-mL beaker at 20 °C. The mixture was kept for 30 min until the complete dissolution of cyclodextrin (the solution acquired a pale yellow color), followed by the addition of epichlorohydrin (0.78 mL, 10 mmol) and stirring for another 12 h. The reaction mixture, appearing as a transparent aqueous solution of a polymer, was transferred into a 1-L beaker, the residues were rinsed with distilled water (10 mL). Acetone (350 mL) was added to the solution to completely stop the reaction. The solution became cloudy, then it was neutralized by adding concentrated HCl (0.3 mL). The volatile components were removed on a rotary evaporator, the residue was dissolved in distilled water (5 mL) and cooled to 0 °C. The obtained precipitate, a sticky waxy substance with a pale yellow color, was separated by decantation and dried on a rotary evaporator. To remove the absorbed water from the polymer, the precipitate was additionally treated with acetone and diethyl ether at the drying stage. A milky white powder was obtained, the yield was 1.56 g (91.5%). ^{1}H NMR (D_2O), δ: 4.90—4.89 (br.d, 7 H, HC(1)); 3.92—3.56 (br.m, 41 H, HC(5),C(6), $OCH_2C\underline{H}(OH)CH_2O$, $OC\underline{H}_2CH(OH)C\underline{H}_2O$); 3.56—3.30 (br.m, 22 H, HC(2),C(3),C(4)). ^{13}C NMR (D_2O), δ: 101.86 (C(1)); 81.09 (C(4)); 73.10 (C(2)); 72.05 (C(3), C(5)); 71.84 ($OCH_2\underline{C}H(OH)CH_2O$, $O\underline{C}H_2CH(OH)\underline{C}H_2O$); 62.50 ($OCH_2CH(OH)\underline{C}H_2OH$); 60.23 (C(6)). IR, ν/cm^{-1}: 3490—3080 (O—H_{st}), 2924 (C—H_{st}), 2395—2287 (CO_{2st}), 1875—1630 (H—O—$H_{\delta,ads}$, C—O—H...O_δ); 1456 ($CH_{2\delta}$, C—$H_{\delta,as}$); 1375 (C—$H_{\delta,sy}$), 1155 (CH—OH_{st}), 1065—955 (C—O—C_{st}), 839 ($CH_{2\gamma}$). MALDI MS, *m/z* (I_{rel} (%)): 1157.359 [β-CD + Na]$^+$ (100), 1179.255 [β-CD + 2 Na – H]$^+$ (19), 1201.194 [β-CD + 3 Na – 2 H]$^+$ (7), 1213.409 [β-CD-Glycd – H_2O + + Na]$^+$ (68), 1231.387 [β-CD-Glycd + Na]$^+$ (73), 1253.213 [β-CD-Glycd + 2 Na – H]$^+$ (17), 1269.921 [β-CD-Glycd + 2 Na – H + H_2O]$^+$, [β-CD-$Glycd_2$ – – 2 H_2O + Na]$^+$ (13); 1275.420 [β-CD-Glycd + 3 Na – – 2 H]$^+$ (6), 1287.448 [β-CD-$Glycd_2$ – H_2O + Na]$^+$ (39), 1305.443 [β-CD-$Glycd_2$ + Na]$^+$ (22), 1328.000 [β-CD-$Glycd_2$ + 2 Na – H]$^+$ (10), 1343.925 [β-CD-$Glycd_2$ + + 2 Na – H + H_2O]$^+$, [β-CD-$Glycd_3$ – 2 H_2O + Na]$^+$ (6); 1350.475 [β-CD-$Glycd_3$ – 3 H_2O + 2 Na – H]$^+$ (2), 1361.511 [β-CD-$Glycd_3$ – H_2O + Na]$^+$, [β-CD-$Glycd_2$ + + 2 Na – H + 2 H_2O]$^+$ (8); 1384.316 [β-CD-$Glycd_3$ – – H_2O + 2 Na – H]$^+$, [β-CD-$Glycd_2$ + 3 Na – 2 H + + 2 H_2O]$^+$ (6); 1403.24 [β-CD-$Glycd_2$ + 3 Na – 2 H + + 3 H_2O]$^+$, [β-CD-$Glycd_3$ + 2 Na – H]$^+$ (4); 1417.945 [β-CD-$Glycd_4$ – 2 H_2O + Na]$^+$, [β-CD-$Glycd_3$ + 2 Na – – H + H_2O]$^+$ (1); 1436.079 [β-CD-$Glycd_4$ – H_2O + Na]$^+$ (1); 1458.795 [β-CD-$Glycd_4$ – H_2O + 2 Na – H]$^+$ (2); 2347.810 [β-CD_2-Glycd – H_2O + Na]$^+$ (4); 2403.781 [β-CD_2-$Glycd_2$ – 2 H_2O + Na]$^+$ (5); 2423.036 [β-CD_2-$Glycd_2$ – H_2O + Na]$^+$ (6); 2445.759 [β-CD_2-$Glycd_2$ – – H_2O + 2 Na – H]$^+$ (3); 2459.761 [β-CD_2-$Glycd_3$ – – 3 H_2O + Na]$^+$, [β-CD_2-$Glycd_2$ + H_2O + Na]$^+$ (8); 2478.070 [β-CD_2-$Glycd_3$ – 2 H_2O + Na]$^+$ (11); 2497.689 [β-CD_2-$Glycd_3$ – H_2O + Na]$^+$ (9); 2516.538 [β-CD_2-$Glycd_4$ – 4H_2O + Na]$^+$, [β-CD_2-$Glycd_3$ + Na]$^+$ (6); 2533.121 [β-CD_2-$Glycd_4$ – 3 H_2O + Na]$^+$, [β-CD_2-$Glycd_4$ – – 2 H_2O + H]$^+$ (10); 2552.410 [β-CD_2-$Glycd_4$ – 2 H_2O + + Na]$^+$ (9); 2573.129 [β-CD_2-$Glycd_4$ – 2 H_2O + 2 Na – – H]$^+$, [β-CD_2-$Glycd_4$ – H_2O + Na]$^+$ (6); 2589.846 [β-CD_2-$Glycd_4$ + H + 2 H_2O]$^+$, [β-CD_2-$Glycd_5$ – 4 H_2O + + Na]$^+$ (5); 2608.140 [β-CD_2-$Glycd_5$ – 3 H_2O + Na]$^+$ (4); 2626.33 [β-CD_2-$Glycd_5$ – 2 H_2O + Na]$^+$ (7); 2646.420 [β-CD_2-$Glycd_6$ – 6 H_2O + Na]$^+$ (2); 2662.494 [β-CD_2-$Glycd_5$ + Na]$^+$, [β-CD_2-$Glycd_6$ – 4 H_2O + Na]$^+$ (2); 2680.612 [β-CD_2-$Glycd_6$ – 3 H_2O + Na]$^+$ (2).

Synthesis of ruthenium catalyst Ru@β-CD-Glycd based on a water-soluble cyclodextrin-containing polymer was carried out similarly to the procedures.[19,30] Polymer β-CD-Glycd (350 mg) and distilled water (20 mL) were placed in a 50-mL round bottom flask equipped with a magnetic stirrer and a reflux condenser, followed by the addition of $RuCl_3$ (35 mg, 0.17 mmol). The mixture was stirred at 20 °C for 12 h, which was accompanied by a change of the color of the solution from yellow-brown to black-yellow within 2 h. After the completion of the reaction, the water was removed on a rotary evaporator, the residue was washed with acetone and dried in air. The catalyst precursor (370 mg, 96%) was obtained as a black-yellow glassy powder. To reduce Ru^{III} to Ru^0, the above-obtained catalyst precursor and 95% ethanol (10 mL) were placed in a 50-mL round bottom flask equipped with a magnetic stirrer and a reflux condenser. A solution of $NaBH_4$ (65 mg, 1.7 mmol) in distilled water (5 mL) was added dropwise to the suspension at 20 °C with stirring, rinsing the residual solution with water (5 mL). The reaction mixture was stirred for 12 h, during which a gradual evolution of gas was observed. Then, distilled water (10 mL) was added to dissolve the precipitate. The subsequent addition of acetone was accompanied by the evolution of gas and the formation of a black precipitate, which was collected by filtration. The sticky precipitate was dissolved in distilled water (10 mL), dried on a rotary evaporator, washed with 95% ethanol to separate the obtained borax, and dried in air. A glassy black powder was obtained (180 mg, 49%). ICP-AES: 3.27% Ru. XPS (eV): 280.5 (Ru/RuO_x, Ru $3d_{5/2}$, 0.03%); 282.2

(RuO_x/Ru, RuO_2 or $RuCl_3 \cdot xH_2O$, Ru $3d_{5/2}$, 0.35%); 283.0 (RuO_3, Ru $3d_{5/2}$, 0.19%); 284.9 (Ru/RuO_x, Ru $3d_{3/2}$); 286.4 (RuO_x/Ru, RuO_2 or $RuCl_3 \cdot x H_2O$, Ru $3d_{3/2}$); 287.3 (RuO_3, Ru $3d_{3/2}$); 286.3 (—OCH—CH_2OH, —CH(OH)—CH(OH)—, $OCH_2CH(OH)CH_2O$, C 1s, 39.42%); 287.6 (—O—CH—O—, —$CHCH_2OH \rightarrow RuO_x$, C 1s, 12.57%); 291.0 (C 1s sat); 461.6 (Ru/RuO_x, Ru $3p_{3/2}$); 464.3 (RuO_x/Ru, RuO_2 or $RuCl_3 \cdot xH_2O$, Ru $3p_{3/2}$); 465.8 (RuO_3, Ru $3p_{3/2}$); 530.6 (RuO_x, RuO_2, RuO_3, O 1s, 3.63%); 532.6 (—CH(OH)—CH(OH)—, —C(H)OCH_2-$CH(OH)CH_2OC(H)$—, —C(H)O—CH—OC(H)—, O 1s, 32.45%); 534.2 (—C(H)—O...H_2O...HO—CH—, O 1s, 3.79%); 536.6 ($CHCH_2OH \rightarrow RuO_x$, $H_2O \rightarrow RuO_x$, H_3O^+, O 1s, 7.56%). IR, ν/cm^{-1}: 3600—3010 (O—H_{st}, H_2O); 2960—2815 (C—H_{st}); 1710—1575 (H—O—$H_{\delta,ads}$, C—O—H...O_δ); 1518 ($CH_{2\delta}$, C—$H_{\delta,as}$); 1315 (C—$H_{\delta,sy}$), 1153 (CH—OH_{st}), 1100—885 (C—O—C_{st}), 874, 841 ($CH_{2\gamma}$).

Protocol for the catalytic experiments. The catalyst and substrate in the required ratio were placed into a steel thermostatically controlled autoclave equipped with a glass test-tube insert and a magnetic stirrer. Water was added in a ratio of 1 μL of H_2O per 1 mg (or 1 μL) of the substrate (V(substrate) = V(H_2O)). The autoclave was sealed, filled with hydrogen up to a pressure of 30 atm, and connected to the termostat. The reaction was carried out at a temperature of 95 °C under continuous stirring for the specified reaction time. Then the autoclave was cooled to 10 °C and depressurized.

The reaction products were analyzed by GLC. The hydrogenation products of aromatic compounds were additionally diluted with toluene, while the hydrogenation products of phenols, LA and its esters were diluted with propan-2-ol. The chromatograms were recorded and processed using the Maestro 1.4 program (https://www.gerstelus.com/product/maestro-software/). The conversion (Conv) was determined from the change in the relative areas (S, %) of substrate and reaction product peaks according to the formula:

$$\mathrm{Conv} = \frac{\sum_i S_{pi}}{S_{\mathrm{substr}} + \sum_i S_{pi}} \cdot 100,$$

where S_{substr} is the relative area of the substrate peak, $\sum_i S_{pi}$ is the sum of the relative areas of the peaks of all the reaction products.

The yield of certain hydrogenation product (ω_{pi}) was determined as the ratio of the area of the corresponding peak S_{pi} to the sum of the peak areas of all the reaction products $\sum_i S_{pi}$ (selectivity) taking into account conversion:

$$\omega_{pi} = \mathrm{Conv} \cdot \frac{S_{pi}}{\sum_i S_{pi}} = \frac{S_{pi}}{S_{\mathrm{substr}} + \sum_i S_{pi}} \cdot 100.$$

The catalyst activity, defined as the reaction turnover frequency (TOF), was calculated by the formula:

$$\mathrm{TOF}(H_2) = \frac{v_{\mathrm{substr}} \sum_i (\omega_{pi} k_i)}{v_{\mathrm{Ru}} t},$$

where v_{substr} is the starting amount of the substrate in the reaction (mmol), ω_{pi} is the yield of one of the products in the unit fractions, k_i is the corresponding stoichiometric amount of consumed hydrogen, v_{Ru} is the starting amount of ruthenium in the reaction medium (mmol), t is the minimum reaction time for which conversion was determined.

Experiments on the catalyst reuse were carried out as follows. The catalyst (5 mg, 1.6 μmol of Ru), ethyl levulinate (380 μL, 2.68 mmol), and water (380 μL) were placed into a steel thermostatically controlled autoclave equipped with a glass test-tube insert and a magnetic stirrer, after which the autoclave was sealed, filled with hydrogen to a pressure of 30 atm, and connected to the termostat. The reaction was carried out at a temperature of 95 °C under stirring for 1 h, then the autoclave was cooled to 10 °C and depressurized. Acetone (5 mL) was added to the reaction products in the glass test-tube, and the mixture was allowed to stand for ~30 min. Then the liquid layer was separated by decantation and analyzed by GLC. The catalyst remaining in the test-tube was dried in air to remove residual acetone and used in the next reaction cycle.

Results and Discussion

Water-soluble polymer carrier β-CD-Glycd was obtained by the reaction of β-CD with epichlorohydrin in an aqueous alkaline medium according to the previously described procedure using low concentrations of NaOH (pH ≈ 12—13) (Scheme 1).[23]

Carrying out polycondensation in a large volume of water at room temperature provided not only a complete dissolution of β-CD,[31] but also made it possible to prevent the possibility of gelation.[23] In this case, the NaOH concentration was <1 wt.%, which led to the formation of a linear water-soluble polymer,[23] which was subsequently used to efficiently stabilize ruthenium NPs. According to published results, mainly secondary hydroxyl groups at the C(2) and C(3) atoms of the glucopyranose units in β-CD underwent deprotonation under these conditions.[23] The obtained β-CD-Glycd polymer was characterized by ^{1}H and ^{13}C NMR spectroscopy and MALDI mass spectrometry. The NMR spectra of the β-CD-Glycd carrier are shown in Figs 2 and 3. The β-CD-Glycd polymer carrier was highly soluble in water,

Scheme 1

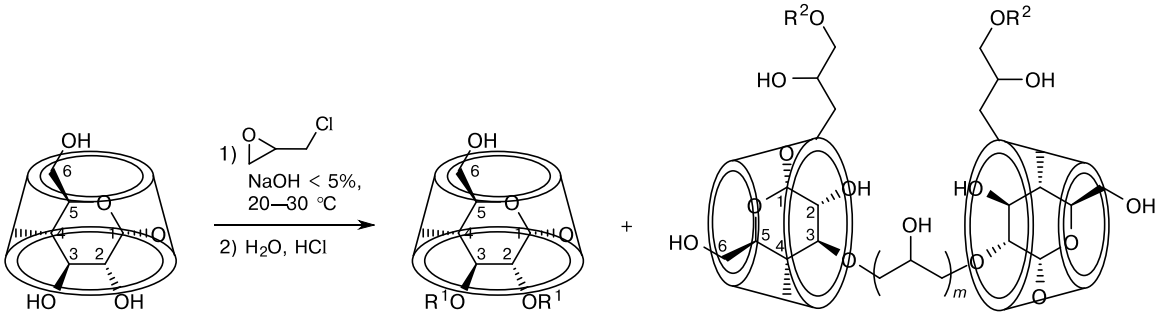

m = 1—4
R^1 = H, $CH_2CH(OH)CH_2OH$, $CH_2CH(OH)CH_2O$-β-CD, $(CH_2CH(OH)CH_2O)_nH$, $(CH_2CH(OH)CH_2O)_n$-β-CD;
R^2 = H, β-CD, $(CH_2CH(OH)CH_2O)_nH$, $(CH_2CH(OH)CH_2O)_n$-β-CD

but insoluble in other polar solvents (DMSO or DMF).

The calculation of the integral intensities of signals in the δ range of 3.92—3.56 for protons both at the C(5) and C(6) atoms in the glucopyranose units of β-CD and in the glycidyl fragments with respect to the integral intensity of the proton signal at the anomeric carbon atom C(1) in the glucopyranose units of β-CD (δ = 4.9—4.8) in the ^{1}H NMR spectrum with water supression in accordance with the procedure[23] showed that there were four glycidyl units per cyclodextrin moiety in the obtained polymer: β-CD : Glycd ≈ 1 : 4 (Table 1).[23,32] A comparison of the obtained ^{13}C NMR spectrum with the results[23] showed the absence of unreacted epoxy groups and the presence of hydrolyzed glycidyl fragments $OCH_2CH(OH)CH_2OH$, along with bridging ones, in the final product (see Fig. 3).

It is important to note that the ratio of the integral intensities of the characteristic protons in the ^{1}H NMR spectrum of the β-CD-Glycd sample (see Fig. 2) shows only the average β-CD/Glycd ratio, since the resulting β-CD-Glycd carrier is a mixture of oligomers. We note that the signals from several different protons are located in the same range simultaneously, which makes it impossible to calculate the spin-spin coupling constants, among other things.

MALDI mass spectrometry (Fig. 4) in the positive ions registration regime (*m*/*z* 200—6000) detected signals whose mass numbers corresponded to cationized products of β-CD polycondensation with epichlorohydrin in the aqueous alkaline medium with the β-CD : Glycd ratio ranging from 2 : 1 to 1 : 4. It

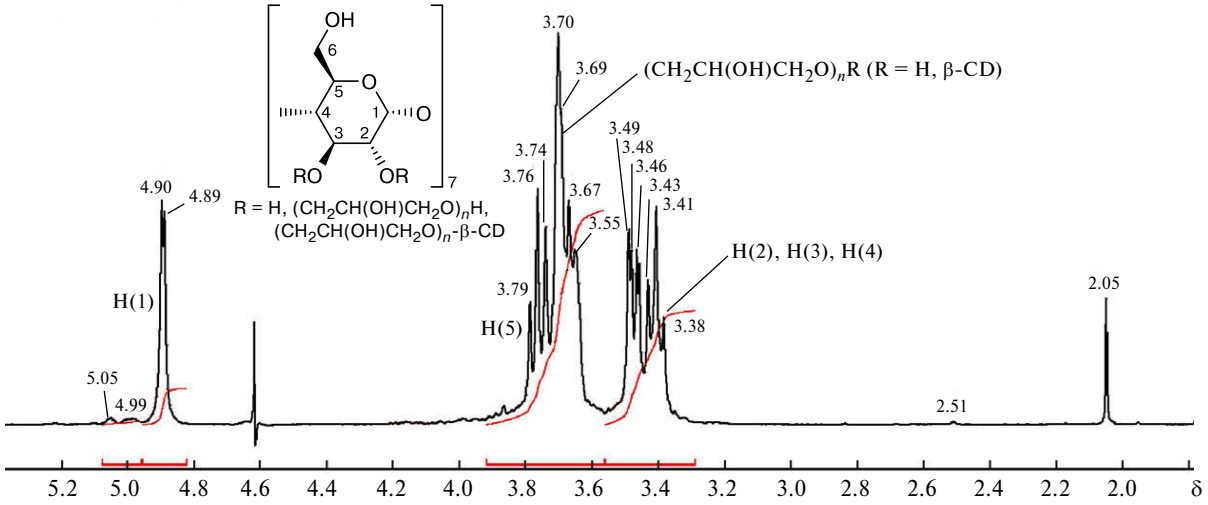

Fig. 2. ^{1}H NMR spectrum of the β-CD copolymer with epichlorohydrin (β-CD-Glycd) in D_2O.

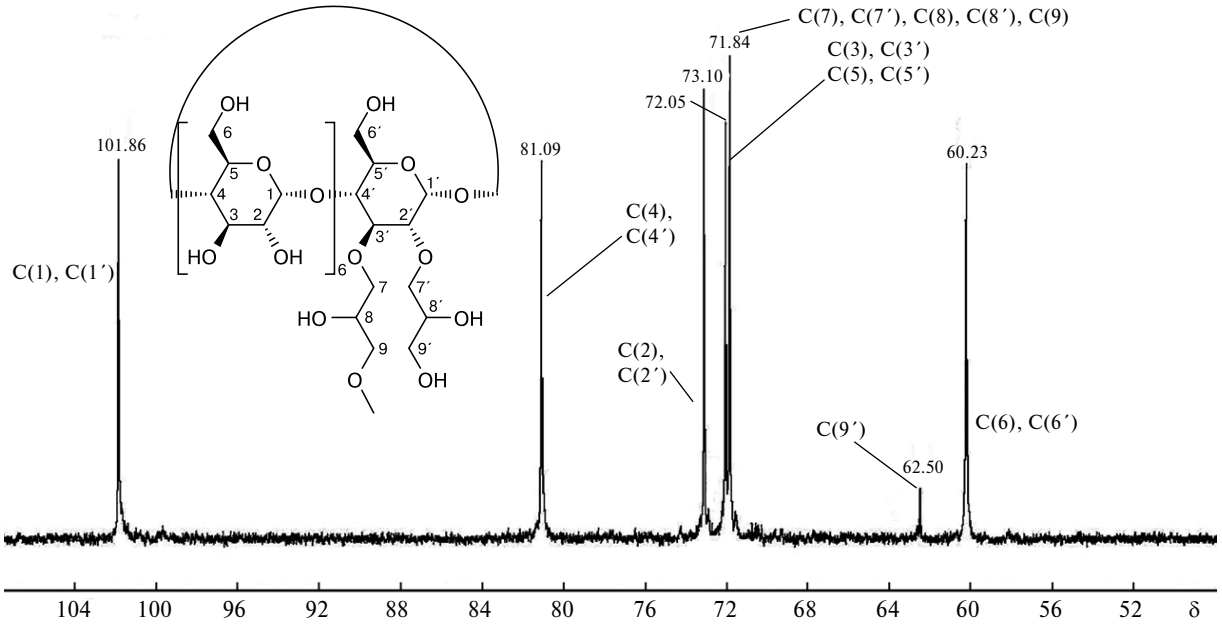

Fig. 3. ^{13}C NMR spectrum of the β-CD copolymer with epichlorohydrin (β-CD-Glycd) in D_2O.

Table 1. Comparison of the integral intensities of proton signals of β-CD and the β-CD-Glycd polymer in the ^1H NMR spectra

Signal	δ	β-CD[a]	Signal	δ	β-CD-Glycd[b]
HC(1)	4.80	7 H	HC(1)	4.91—4.90	7 H
HC(5), HC(6)	3.68—3.55	21 H	HC(5), HC(6), $OCH_2C\underline{H}(OH)CH_2O$, $OC\underline{H}_2CH(OH)C\underline{H}_2O$	3.92—3.56	41 H
HC(3)	3.65—3.46	7 H	HC(2), HC(3), HC(4)	3.56—3.30	22 H
HC(2), HC(4)	3.38—3.22	14 H			

[a] In DMSO-d_6.
[b] In D_2O.

should be noted that under analysis conditions, upon heating under the action of laser radiation, both depolymerization and dehydration of the sample occur, resulting the formation of epoxy cycles in the glycidyl moieties (Scheme 2).[33] As a consequence, the products of depolymerization are those undergoing desorption/ionization. Therefore, MALDI mass spectrometry does not allow us to unambigu-

Scheme 2

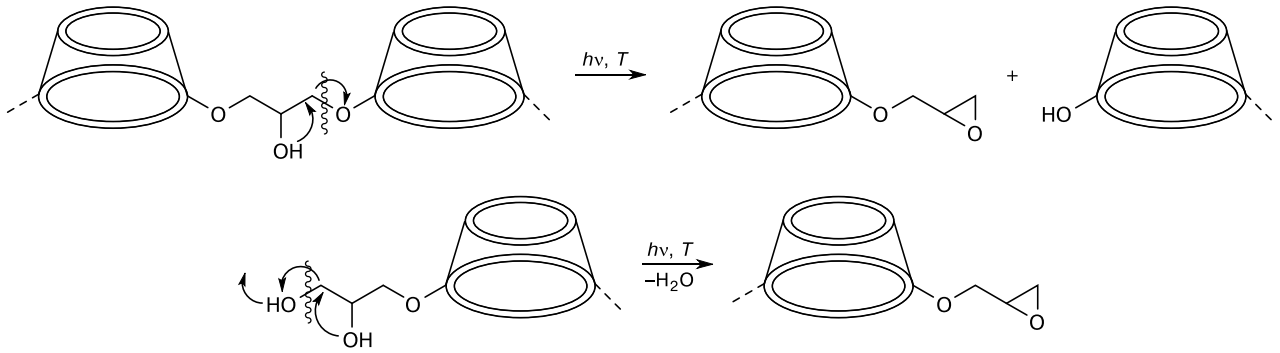

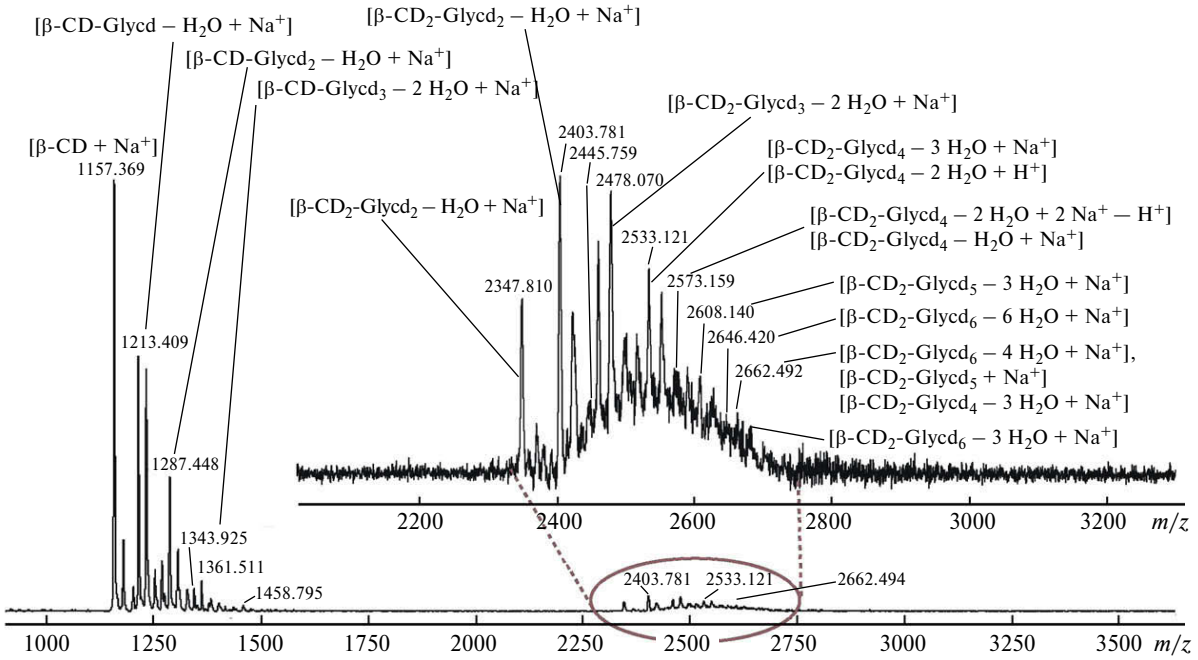

Fig. 4. MALDI mass spectrum of the β-CD-Glycd.

ously determine the predominance of a particular compound in the sample exclusively from the relative integral intensity of the corresponding signals, hence being mostly qualitative method of analysis.

It was shown previously[33] for β-CD modified with polyglycidyl, whose number-average molecular weight M_n and the weight-average molecular weight M_w, according to gel-permeation chromatography, were 2180 and 3950 Da, respectively MALDI mass spectrometry did not register polycondensation products with $m/z > 1899$, while peaks with m/z of 1603 and 1677 being the strongest. According to the work,[23] the maximum weight-average molecular weight M_w for the water-soluble linear β-CD copolymer with epichlorohydrin obtained by this method can reach 5000—6000 Da. Moreover, at best, trimers and tetramers are identified in the MALDI mass spectra. Thus, the MALDI method can be used to determine the content of unmodified cyclodextrin only approximately. Even taking into account the available data on the total area of the peaks, this value does not exceed 10%.

Synthesis of ruthenium nanocatalyst based on a cyclodextrin-containing polymer β-CD-Glycd was carried out by analogy with the procedure.[19] The interaction of the β-CD-Glycd polymer carrier with $RuCl_3$ and the subsequent reduction of Ru^{III} to Ru^0 in the presence of $NaBH_4$ at room temperature in an aqueous medium led to the formation of a Ru@β-CD-Glycd nanocatalyst (Scheme 3). The driving force of this reaction was the formation of complexes between Ru^{3+} ions and hydroxyl groups of β-cyclodextrin moieties.[34—36] Further stabilization of the resulting NPs was also achieved through the interaction of surface ruthenium atoms with both primary and secondary donor hydroxyl groups of cyclodextrin[19] and glycidyl fragments.[22,37] Like the starting polymer, the synthesized Ru@β-CD-Glycd nanocatalyst dissolved in water and formed a separate phase in ethanol.

It should be noted that the above scheme reflects the stabilization of Ru NPs as rather suggestive. For example, it was reported[19] that for the steric stabilization of Ru NPs with diameters of about 1.5 nm by individual CD, the molar CD/Ru ratio should be higher than 3, moreover, it was noted that an excess of cyclodextrin was necessary for an effective transfer of the substrate between the organic and aqueous phases. In our case, β-CD polymers are linked into the chain by glycidyl bridges, which can also take part in the stabilization of ruthenium NPs. As a result, the β-CD/Ru ratio may differ for each individual particle of a similar size, and cyclodextrin moieties belonging to the different chains of the obtained polymer can be involved in the stabilization of a single NP.

Scheme 3

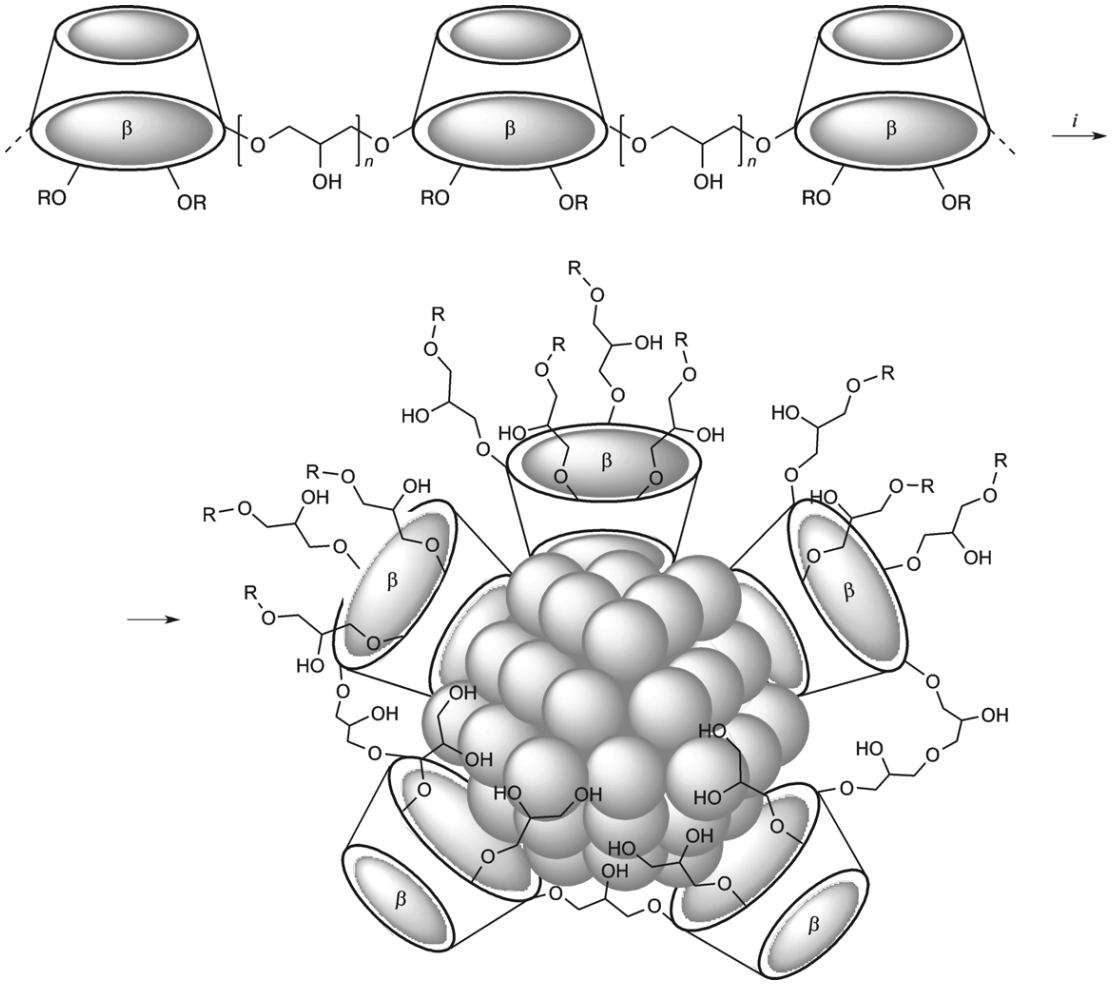

n = 1—4; R = H, $CH_2CH(OH)CH_2OH$, $CH_2CH(OH)CH_2O$-β-CD

Reagents and conditions: *i*. 1) $RuCl_3$, H_2O, 20 °C, 12 h; 2) $NaBH_4$, H_2O, EtOH, 20 °C, 12 h.

The obtained Ru@β-CD-Glycd nanocatalyst was characterized using TEM, XPS, SAXS, and ICP-AES (Figs 5—8).

It was determined that the Ru@β-CD-Glycd sample consisted of highly dispersed, uniformly distributed particles (Fig. 5). The average particle

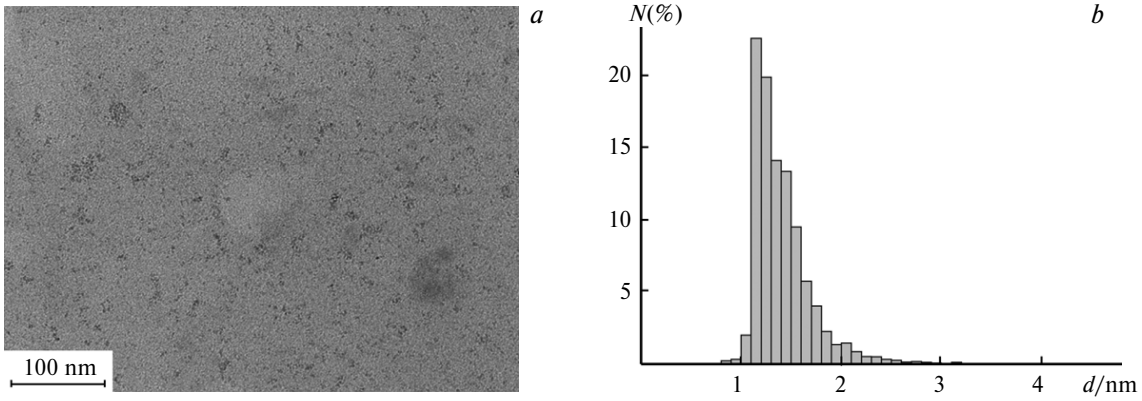

Fig. 5. TEM image and particle size distribution histogram for the Ru@β-CD-Glycd nanocatalyst.

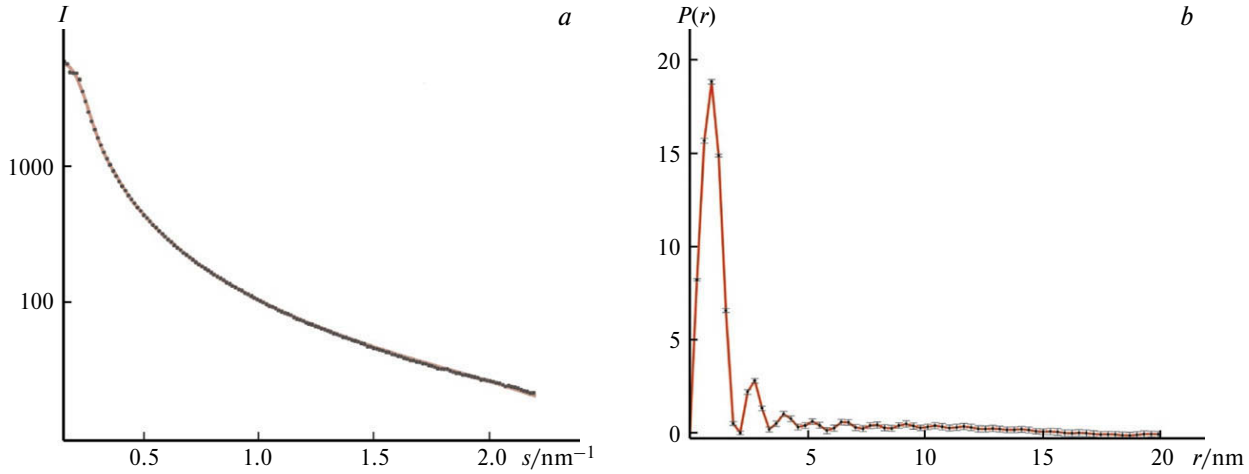

Fig. 6. X-ray scattering intensity *s* at small angles (*a*) and pair size distribution function (*b*) for the Ru@β-CD-Glycd nanocatalyst.

sizes calculated using TEM (see Fig. 5) and SAXS results (see Fig. 6) were 1.41 and 0.92 nm, respectively. The discrepancy in the obtained results can be explained by the limited resolution of TEM. Nevertheless, according to TEM date, 57% of the particles belong to the fraction of particles with sizes of 1.1—1.3 nm, which is in agreement not only with the results of the work[19] on the synthesis of Ru NPs stabilized with methylated cyclodextrins, but also with the SAXS results. This small size of Ru NPs may be due to the high β-CD content in the polymer carrier with relatively short glycidyl bridges and, as a consequence, the predominant role of cyclodextrins in the stabilization of NPs. Thus, when PEG diglycidyl ether was used as a cross-linking agent for β-CD and polypropylenimine (PPI) dendrimers, the average particle size after the synthesis under similar conditions (H_2O, 0—20 °C) was 1.7—2.2 nm.[22,37]

Based on the results of ICP-AES, the Ru content in the Ru@β-CD-Glycd sample was 3.27 wt.%. According to XPS data, the surface atomic concentrations of elements were (at.%): Ru — 0.57, C — 51.99, and O — 47.44. Table 2 gives the oxidation states of Ru and the bond energies (*E*) on the sample surface.

The XPS did not reveal boron (B 1s, 188—193 eV) or chlorine (Cl 2p, 198—203 eV) compounds were

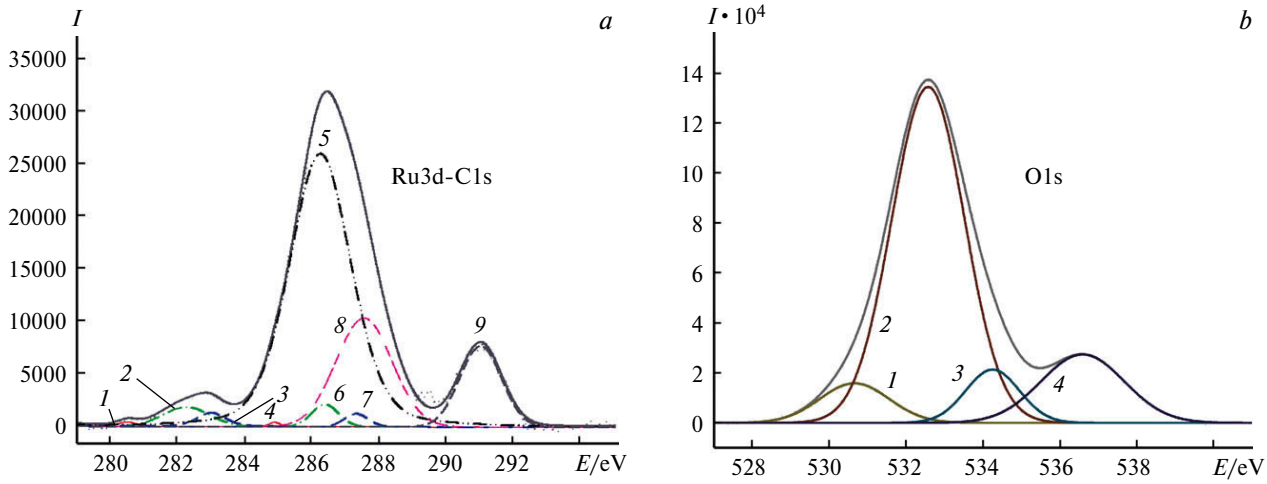

Fig. 7. X-ray photoelectron spectra of the Ru@β-CD-Glycd nanocatalyst: (*a*) deconvolution of Ru 3d and C 1s lines: Ru/RuO_x, Ru $3d_{5/2}$ (*1*), RuO_x/Ru, RuO_2, $RuCl_3 \cdot x\,H_2O$, Ru $3d_{5/2}$ (*2*), RuO_3, Ru $3d_{5/2}$ (*3*), Ru/RuO_x, Ru $3d_{3/2}$ (*4*), —CH(OH)—CH(OH)—, $OCH_2CH(OH)CH_2O$, C 1s (*5*), RuO_x/Ru, RuO_2, $RuCl_3 \cdot x\,H_2O$, Ru $3d_{3/2}$ (*6*), RuO_3, Ru $3d_{3/2}$ (*7*), —O—CH—O—, —$CHCH_2OH \rightarrow RuO_x$, C 1s (*8*), C 1s sat (*9*); (*b*) deconvolution of O 1s line: RuO_x, RuO_2, RuO_3 (*1*), —CH(OH)—CH(OH)—, —$C(H)OCH_2CH(OH)CH_2OC(H)$— (*2*), —C(H)—O...H_2O...HO—CH— (*3*), $CHCH_2OH \rightarrow RuO_x$, $H_2O \rightarrow RuO_x$, H_3O^+ (*4*).

Table 2. Ruthenium oxidation states on the surface of the Ru@β-CD-Glycd nanocatalyst sample based on XPS spectra*

State	Ru (%)	*E*/eV
Ru/RuO_x	5.1	280.5
RuO_x /Ru, RuO_2, $RuCl_3 \cdot xH_2O$	62.0	282.2
RuO_3	32.9	283.0

* Fraction of Ru $3d_{5/2}$ atoms (%) in the oxidation state, characterized by the corresponding binding energy (eV).

present on the surface of the Ru@β-CD-Glycd sample. Therefore, the obtained sample did not contain NaCl, $NaBO_2$, Na_3BO_3, or $Na_2B_4O_7$ impurities being formed during catalyst synthesis and reduction of Ru NPs from $RuCl_3$ in the presence of $NaBH_4$. Ruthenium was found mainly in the form of surface oxides:[38—40] RuO_x, RuO_2, RuO_3 (see Table 2, Fig. 7, *a*), which were previously observed for Ru catalysts based on polypropylenimine dendrimers cross-linked with PEG diglycidyl ether.[37] Accordingly, the presence of RuO_2 and, especially, RuO_3 in the XPS spectrum of the Ru@β-CD-Glycd catalyst can be explained by the interaction of surface ruthenium atoms with hydroxyl groups of the β-CD moieties[37] and absorbed water contained in the cyclodextrin,[15,41] the peak of which is clearly visible in the O 1s spectrum (see Fig. 7, *b*).[41] The low surface ruthenium content (0.57%) may be due to the shielding of Ru NPs by β-CD moieties. This assumption is indirectly confirmed by the relatively low (7.7%) fraction of ruthenium oxides in the O 1s spectrum.

In the C 1s spectrum, an increased contribution of the signal corresponding to anomeric carbon atoms C(1) in the glucopyranose units of β-CD to the total intensity is observed (see Fig. 7, *a*).[42—44] This can be explained by a shift of the electron density from carbon to oxygen and from oxygen to ruthenium at stabilization of NPs: $—C(H)^{\delta+} \rightarrow O \rightarrow Ru$, $—CH_2^{\delta+} \rightarrow O \rightarrow Ru$. According to XPS and IR spectroscopy data, the oxidation of primary CH_2OH groups into aldehyde groups did not occur. Thus, the XPS spectrum of the O 1s line (see Fig. 7, *b*) clearly shows a peak with a maximum at a binding energy of 532.6 eV, corresponding to single —CH—OH bonds in the glycosidic units of the cyclodextrin moieties,[42—44] but not C=O bonds (531.0—531.7 eV).[44]

In turn, the IR spectra of the starting β-CD and the Ru@β-CD-Glycd nanocatalyst showed the almost complete overlap of the bands characteristic of the C—O and O—H bonds (see Fig. 8). The band at 1700—1550 cm^{-1} in both spectra with maxima at

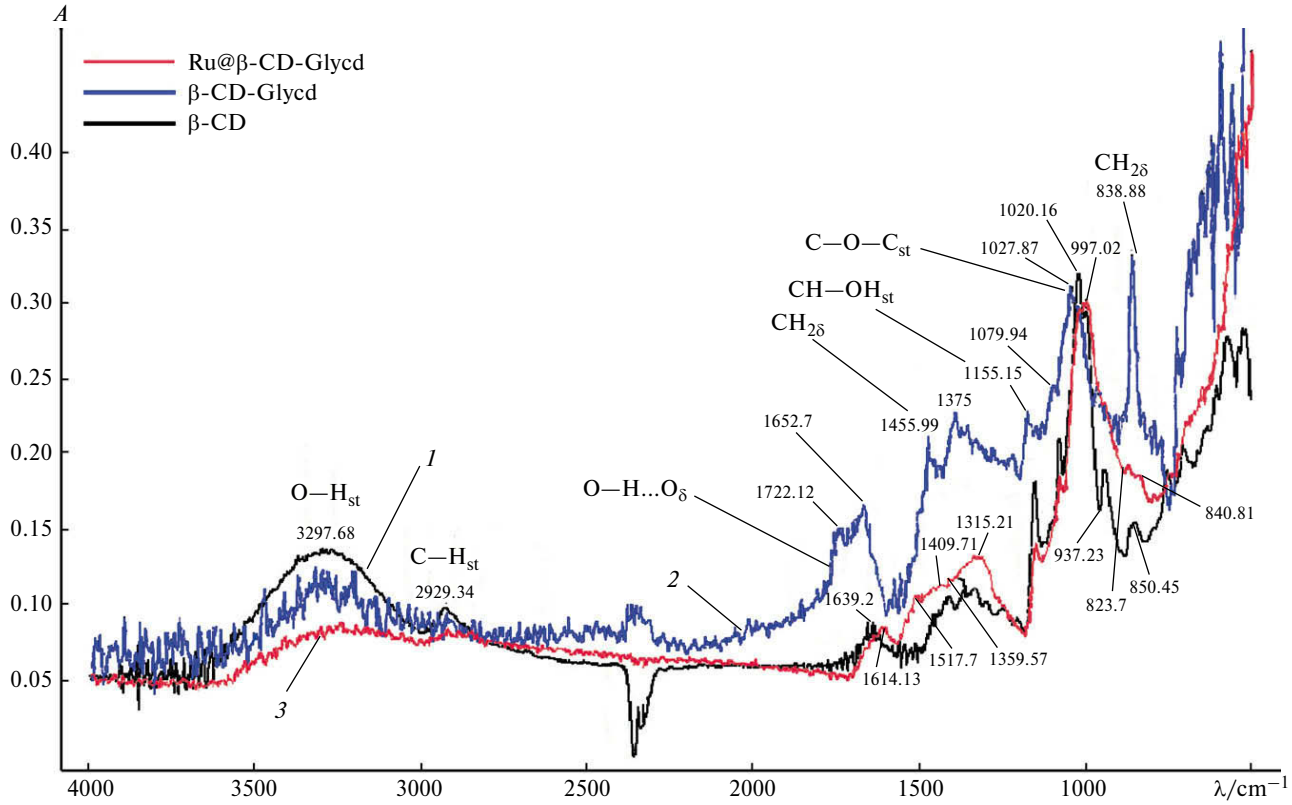

Fig. 8. IR spectra of β-CD (*1*, black), β-CD-Glycd polymer carrier (*2*, blue), and Ru@β-CD-Glycd catalyst (*3*, red).

1639 and 1614 cm^{-1} refers to bending vibrations of H—O—H bonds in the absorbed water molecules and C—O—H bonds in the β-CD hydroxyl groups, respectively.[45,46] The spectrum of the starting β-CD also shows well-resolved bands at 2929 cm^{-1} and 937 cm^{-1}, corresponding to asymmetric stretching vibrations of CH_2 groups and bending vibrations of α-(1→4) of glucopyranose rings, respectively.[22]

On the contrary, the spectrum of the β-CD-Glycd polymer carrier exhibited a noticeable increase in intensity and a shift to higher wavenumbers for the bands corresponding to the stretching vibrations of C—O—C bonds and the bending vibrations of H—O—H and C—O—H bonds (maximum at 1653 cm^{-1}), as well as of CH_2 groups (maxima at 1456 and 1375 cm^{-1}) (see Fig. 8). This is related to the introduction of Glycd fragments into the structure of the polymer sample and, as a result, the subsequent change in the structure of the hydrogen bonds.[22] The band with a maximum at 1722 cm^{-1} can be attributed to the residual impurities of acetone used to precipitate the polymer and retained in it due to hydrogen bonds and hydrophobic interactions.

In contrast to the polymer based on β-CD cross-linked with a long PEG diglycidyl ether,[22] the subsequent inclusion of Ru NPs into the structure of the β-CD-Glycd polymer carrier, the synthesis of which was carried out using short epichlorohydrin, and the transfer of electron density C→O→Ru at NP stabilization led to the next change in the structure of the hydrogen bonds and partial fixation of the polymer carrier fragments around the NPs. In the spectrum, this was reflected by the shift of the bands corresponding to stretching vibrations of C—O—C bonds and bending vibrations of H—O—H and C—O—H bonds to the region of lower wavenumbers, as well as by a sharp drop in the intensity of the bands corresponding to bending vibrations of H—O—H and C—O—H bonds and CH_2 groups (see Fig. 8).

Hydrogenation of unsaturated compounds in the presence of the Ru@β-CD-Glycd catalyst. The influence of the CD-binding effect in the catalyst structure on the hydrogenation efficiency and selectivity in an aqueous medium was investigated using aromatic compounds, phenols, LA and its esters as examples. Under the reaction conditions, Ru@β-CD-Glycd exhibited the properties of a pseudo-homogeneous catalyst. The results on the hydrogenation of benzene, biphenyl, and *trans*-stilbene are given in Table 3.

As seen from Table 3, benzene (**1**) does not undergo hydrogenation in the presence of the Ru@β-CD-Glycd catalyst even at a temperature of 95 °C

Table 3. Hydrogenation of aromatic and unsaturated compounds in the presence of the Ru@β-CD-Glycd catalyst*

Conditions		Conversion (%)	TOF (H_2)/h^{-1}	Products	Selectivity (%)
v_{substr} : v_{Ru}	t/h				
			Substrate — benzene (**1**)		
1740 : 1	2.0	0	0	—	—
			Substrate — biphenyl (**2**)		
1200 : 1	0.5	33.0	2385	Cyclohexylbenzene (**3**) + bicyclohexylidene (**4**) + bicyclohexyl (**5**)	99.8 (**3**), 0.1 (**4**), 0.1 (**5**)
	2.0	99.5	—	**3** + **4** + **5** + **1**	99.25 (**3**), 0.25 (**4**), 0.25 (**5**), 0.25 (**1**)
	6.0	99.5	—	**3** + **4** + **5** + **1**	94.5 (**3**), 1.5 (**4**), 2.0 (**5**), 1.0 (**1**)
			Substrate — *trans*-stilbene (**6**)		
1370 : 1	0.5	33.0	2680	Bicyclohexylethane (**7**) + phenylcyclohexylethane (**8**) + diphenylethane (**9**) + phenylcyclohexenylethane (**10**) + *trans*-β-cyclohexenylstyrene (**11**)	84.09 (**9**), 7.5 (**8**), 7.5 (**10**), 0.5 (**7**), 0.5 (**11**)
	6.0	97.5	—	**7** + **8** + **9** + **10** + **11**	39.5 (**10**), 34.0 (**9**), 23.0 (**8**), 3.0 (**11**), 0.5 (**7**)
	12.0	98.0	—	**7** + **8** + **9** + **10** + **11**	36.0 (**10**), 32.0 (**9**), 24.5 (**8**), 2.5 (**11**), 5.0 (**7**)

*Reaction conditions: 5 mg of cat., 95 °C, 30 atm of H_2, V(substrate) = $V(H_2O)$. Here and in Tables 4 and 5 v_{substr} : v_{Ru} is the substrate : Ru molar ratio.

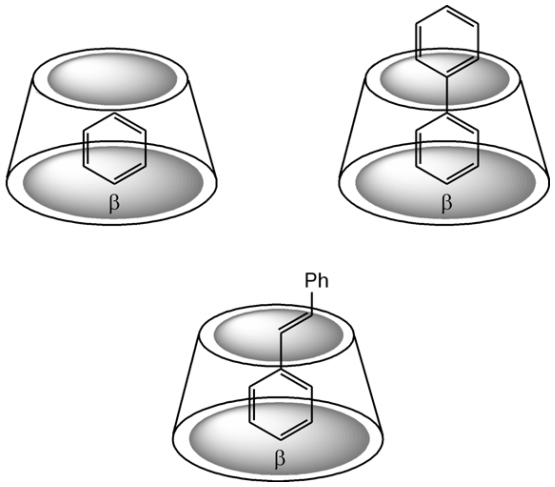

Fig. 9. Inclusion complexes of benzene (**1**), biphenyl (**2**), and *trans*-stilbene (**3**) with β-CD.

and a hydrogen pressure of 30 atm, which essentially distinguishes this catalytic system from Ru catalysts based on networks of polypropylenimine dendrimers,[47,48] providing the exhaustive hydrogenation of aromatic compounds and close to quantitative yields at a temperature of 85 °C and a hydrogen pressure of 5—10 atm under two-phase conditions.[48]

It appears that the formation of a host—guest benzene complex with a β-CD moiety in an aqueous medium (Fig. 9) interferes with hydrogenation.[19,49] Therefore, it can be assumed that in the highly polar medium used (water + β-CD moieties linked by glycidyl bridges), benzene molecules prefer to be located in the hydrophobic cavities of β-CD,[25] and thus avoid hydrogenation.

In particular, a similar effect was observed earlier when using Ru NPs stabilized with β-CD cross-linked with PEG diglycidyl ether[22] or methylated α- and β-CD,[19] which was explained by increased stability constants for the corresponding inclusion complexes.[22,49]

In the case of bulky substrates containing two aromatic moieties (see Fig. 9), only one benzene ring is involved in the formation of the inclusion complex, providing the selectivity hydrogenation of the second aromatic ring only. Thus, biphenyl (**2**) was almost completely converted to cyclohexylbenzene (**3**) within 2 h (see Table 3), however, its further hydrogenation to bicyclohexyl (**5**), in contrast to traditional catalysts such as Ru/C,[50,51] proceeds with difficulty: its fraction among the reaction products was only 2% for a conversion of 99.5% over 6 h (see Table 3). This can be explained by the considerably higher stability constant of the host—guest complexes for the phenyl moiety as compared to the cyclohexyl one.

Among the other products of hydrogenation of biphenyl, small amounts of bicyclohexylidene (**4**) and benzene (**1**) were found. Apparently, a stepwise hydrogenation through the intermediate formation of a cycloalkene fragment also takes place in this case.[50,52] Bicyclohexylidene is formed by the migration of the C=C double bond in 1-cyclohexylcyclohexene (**12**) (Scheme 4). Benzene, in turn, is formed by the hydrogenolysis of biphenyl.[50,52,53]

Hydrogenation of *trans*-stilbene (**6**) in an aqueous medium in the presence of the Ru@β-CD-Glycd catalyst proceeded stepwise in accordance with Scheme 5. First of all, the C=C double bond located outside the CD cavity was subjected to hydrogenation (Fig. 10): after 30 min, the portion of diphenylethane (**9**) among the reaction products was 84% at a conversion of 33%. Further hydrogenation of stilbene led not only to the exhaustive saturation of the C=C double bond (96% conversion over 1 h), but also to the simultaneous saturation of one of the aromatic

Scheme 4

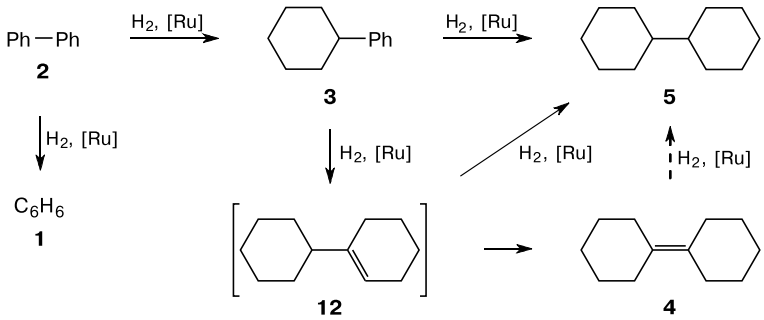

Scheme 5

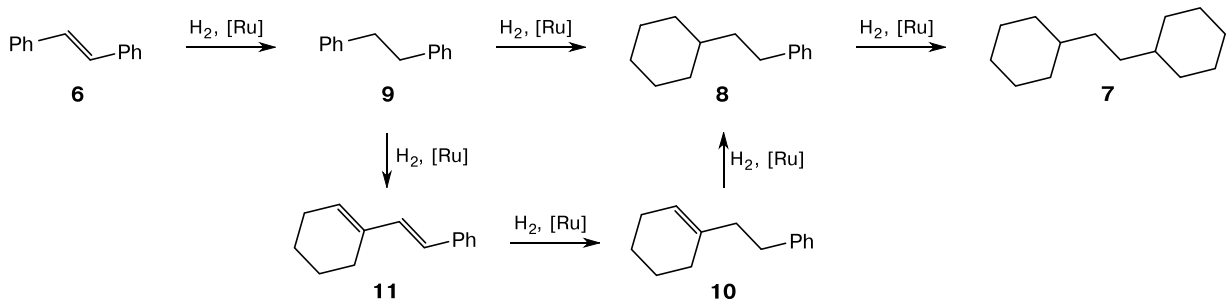

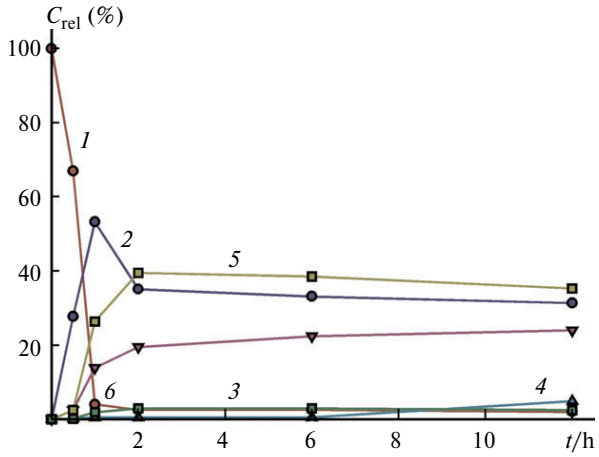

Fig. 10. Changes in relative concentrations (C_{rel}) of *trans*-stilbene (*1*) and products of its hydrogenation (compounds **9** (*2*), **8** (*3*), **7** (*4*), **10** (*5*), **11** (*6*)) over time in the presence of the Ru@β-CD-Glycd catalyst; reaction conditions: 400 mg of stilbene, 5 mg of catalyst (substrate/Ru ≈ 1370), 400 μL of H_2O, 30 atm of H_2, 95 °C.

rings in the formed molecules of diphenylethane (**9**) (the portion of phenylcyclohexylethane among the reaction products increased from 7.5% in half an hour to 23% over 6 h).

We also observed the formation of a small amount of intermediate products of hydrogenation of diphenylethane (**9**), namely, phenylcyclohexenylethane (**10**) and *trans*-β-cyclohexenylstyrene (**11**), which have C=C double bonds in the side chain. Unlike the traditional ruthenium-containing catalysts, no hydrogenation of the second aromatic ring was observed in the presence of the synthesized catalyst Ru@β-CD-Glycd, which can be explained by the strong binding of the aromatic ring by the cavity of the CD moiety.[22,25]

The results of hydrogenation of phenols are given in Table 4. The main product of phenol (**13**) hydrogenation was cyclohexanol (**14**), which is typical of Ru catalysts.[50,51] Even at incomplete conversion, the total fraction of products of incomplete hydrogenation (cyclohexanone **15** + cyclohexen-2-one **16**) did not exceed 2.5% (see Table 4). It can be assumed that the water-soluble phenol, forming hy-

Table 4. Hydrogenation of phenols in the presence of the Ru@β-CD-Glycd catalyst[a]

$v_{substr} : v_{Ru}$	*t*/h	Conversion (%)	TOF (H_2)/h^{-1}	Products	Selectivity (%)
			Substrate — phenol (**13**)		
1970 : 1	0.5	70.5	8250	Cyclohexanol (**14**) + cyclohexanone (**15**) + cyclohexen-2-one (**16**)	97.5 (**14**), 2.0 (**15**), 0.5 (**16**)
	2	100	—	**14**	100
			Substrate — 4-*tert*-butylphenol (**17**)		
2055 : 1	0.5	44.0	5020	*cis*-4-*tert*-Butylcyclohexanol (**18**) + *trans*-4-*tert*-butylcyclohexanol (**19**) + 4-*tert*-butylcyclohexanone (**20**) + **13** + *tert*-butylbenzene (**21**)	48.0 (**18**), 33.0 (**19**), 16.5 (**20**), 1.5 (**21**), 1.0 (**13**)
	6.0	94.0	—	**13** + **18** + **19** + **20** + **21**	50.5 (**18**), 38.5 (**19**), 18.0 (**20**), 2.5 (**21**), 0.5 (**13**)

* Reaction conditions: 5 mg of cat., 95 °C, 30 atm of H_2, V(substrate) = $V(H_2O)$.

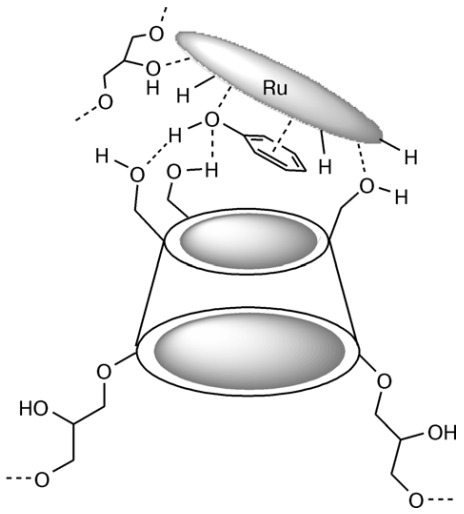

Fig. 11. Adsorption of phenol on the surface of Ru NPs without the complex formation with β-CD.

drogen bonds with hydroxy groups of β-CD and glycidyl chains, was outside the cyclodextrin cavity directly during the reaction, and its relatively small size ensured the possibility of coplanar adsorption on the surface of Ru NPs (Fig. 11). This is characteristic of transition metal NPs stabilized with polyacrylic acid[21] or PPI dendrimers.[30]

Hydrogenation of the more bulky and hydrophobic 4-*tert*-butylphenol (**17**) proceeded elsewise (Scheme 6, see Table 4). A conversion close to quantitative was achieved for this substrate after only 6 h, and among the hydrogenation products there were not only *cis*-4-*tert*-butylcyclohexanol (**18**) and *trans*-4-*tert*-butylcyclohexanol (**19**), but also 4-*tert*-butylcyclohexanone (**20**), a product of incomplete hydrogenation[54] (see Table 4, Fig. 12).

Scheme 6

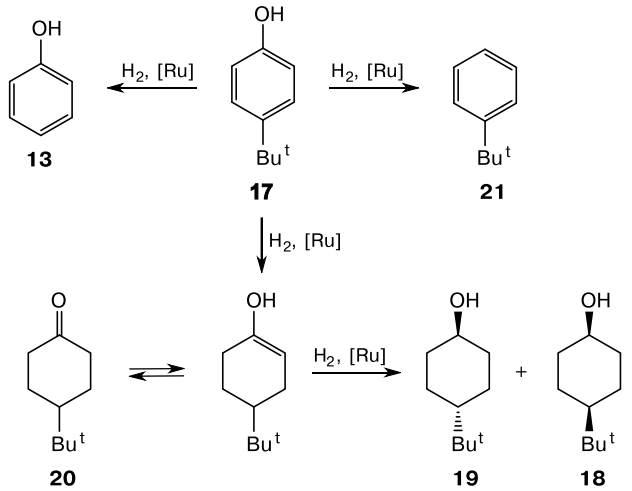

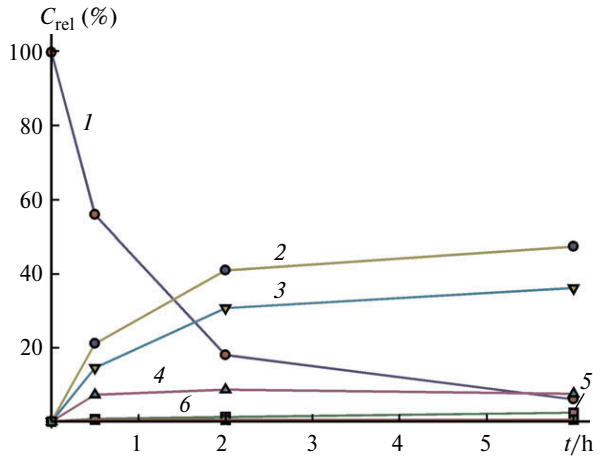

Fig. 12. Change in the relative concentrations of 4-*tert*-butylphenol (*1*) and its hydrogenation products (**18** (*2*), **19** (*3*), **20** (*4*), **21** (*5*), **13** (*6*)) over time in the presence of the Ru@β-CD-Glycd catalyst. Reaction conditions: 500 mg of 4-*tert*-butylphenol, 5 mg of catalyst (substrate/Ru ≈ 2055), 500 μL of H_2O, 30 atm of H_2, 95 °C.

This fact can be explained by the considerably higher stability of the complex of 4-*tert*-butylphenol (**17**) with β-CD moieties, where the cavity of the latter contains a *tert*-butyl substituent and only a part of the aromatic ring (Fig. 13),[55,56] which leads to deceleration of the reaction and the formation of products of incomplete hydrogenation.

Hydrogenation of LA and its esters in the presence of the Ru@β-CD-Glycd catalyst proceeded selec-

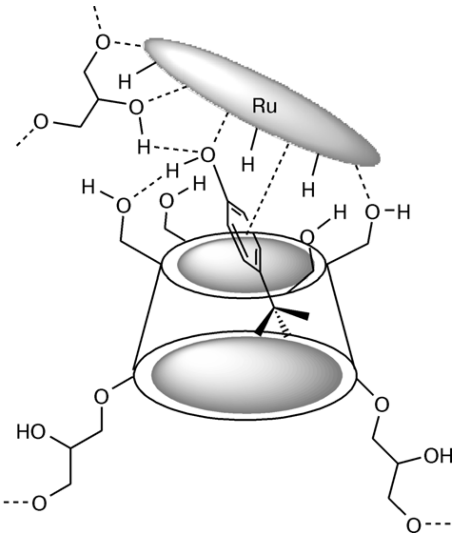

Fig. 13. Adsorption of 4-*tert*-butylphenol (**17**) on the surface of Ru NPs with the formation of an inclusion complex with β-CD.[55,56]

Table 5. Hydrogenation of levulinic acid (LA) and its esters in the presence of the Ru@β-CD-Glycd catalyst*

$v_{substr} : v_{Ru}$	*t*/h	Conversion (%)	TOF (H_2)/h^{-1}	Products	Selectivity (%)	
					γ-VL	angelica lactone (**22**)
			Substrate — LA			
1830 : 1	0.5	100.0	3640	γ-VL + **22**	99.5	0.5
	2.0	100.0	—	γ-VL	100.0	—
3045 : 1	0.5	100.0	6035	γ-VL + **22**	99.0	1.0
9140 : 1	0.5	100.0	1280	γ-VL + **22**	70.0	30.0
	1.0	100.0	—	γ-VL + **22**	79.0	21.0
	2.0	100.0	—	γ-VL + **22**	83.0	17.0
	6.0	100.0	—	γ-VL + **22**	83.0	17.0
			Substrate — methyl levulinate (**23**)			
1695 : 1	0.5	100.0	3395	γ-VL	100.0	—
	2.0	100.0	—	γ-VL	100.0	—
2830 : 1	0.5	75.0	4220	γ-VL + **22**	99.5	0.5
	1.0	95.5	—	γ-VL	100.0	—
			Substrate — ethyl levulinate (**24**)			
1655 : 1	0.5	79.0	2590	γ-VL + **22**	99.0	1.0
	1.0	99.5	—	γ-VL	100.0	—
	2.0	100.0	—	γ-VL	100.0	—
			Substrate — butyl levulinate (**25**)			
1575 : 1	0.5	25.5	785	γ-VL + **22**	96.0	4.0
	1.0	50.0	—	γ-VL + **22**	98.5	1.5
	2.0	99.5	—	γ-VL	100.0	—

* Reaction conditions: 300 (LA), 340 (**23**), 380 (**24**), or 450 (**25**) μL of the substrate; 5, 3, or 1 mg of the catalyst; 95 °C, 30 atm of H_2, V(substrate) = $V(H_2O)$.

tively with the formation of γ-valerolactone (γ-VL) as the major product, through the stage of cyclic intermediates, angelica lactone **22** (Table 5, Scheme 7). The reaction was accompanied by the hydrolysis of the ester groups. In this case, the presence on the ruthenium surface of polymer fragments, which are prone to form multiple hydrogen bonds with the polar groups of the substrate, apparently, directed the reaction course mainly toward the cyclization of LA into angelica lactones, with both the acid itself and its esters tending to undergo this cyclization.[57]

It was found that quantitative yields of γ-VL could be achieved for all the tested substrates (see Table 5).

Scheme 7

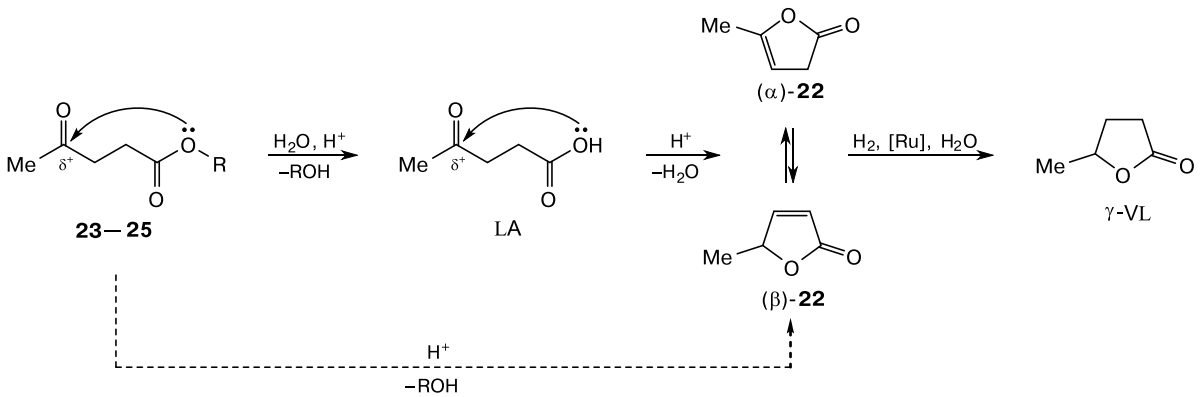

R = Me (**23**), Et (**24**), Bu (**25**)

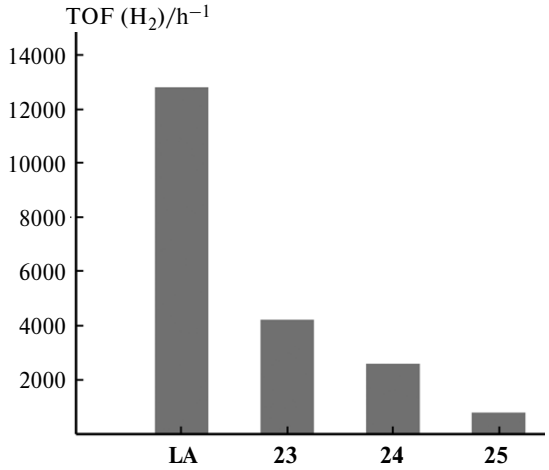

Fig. 14. Comparative hydrogenation of levulinic acid and its esters in the presence of the Ru@β-CD-Glycd nanocatalyst in an aqueous medium; reaction conditions: 95 °C, 30 atm of H_2, V(substrate) = $V(H_2O)$.

The activity of Ru@β-CD-Glycd catalyst in the hydrogenation of the tested substrates, calculated taking into account the amount of absorbed hydrogen (TOF(H_2)), decreased in the order: LA >> **23** > **24** > > **25** (Fig. 14). It can be assumed that LA, like phenol, did not form inclusion complexes with β-CD directly during the reaction, but, due to the formation of hydrogen bonds with hydroxy groups, it was situated above the cavity of the latter (Fig. 15). Thus, the resulting conformation of the substrate facilitated its ready and rapid cyclization into angelica lactones (**22**) and subsequent transformation into γ-VL, the yield of which reached 99—100% over half an hour for a molar ratio substrate/Ru ≈ 3045 (see Table 5).

The introduction of an alkyl substituent into the carboxy group of the substrate led to the formation of inclusion complexes with β-CD moieties (Fig. 16), thereby hindering the hydrogenation. Thus, in the

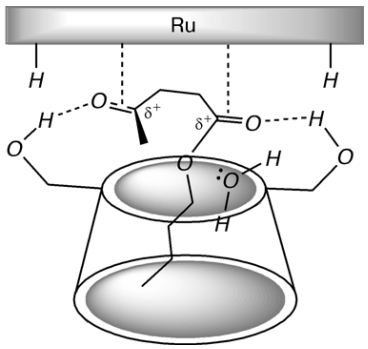

Fig. 15. Interaction of levulinic acid with β-CD hydroxy groups in the presence of Ru NPs.

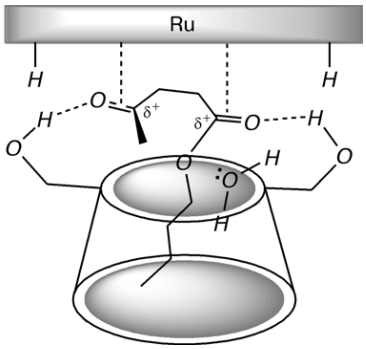

Fig. 16. Formation of an inclusion complex of butyl levulinate (**25**) with β-CD in the presence of Ru NPs.

hydrogenation of LA and its esters for 30 min with a ratio substrate : Ru ≈ 1570—1830, the yield of γ-VL for butyl levulinate (**25**) did not exceed 25%, for ethyl levulinate (**24**) it was 78%, and for methyl levulinate (**23**) and LA it reached 99—100%. Also noteworthy is a particularly high portion of hydrolysis for butyl levulinate: 66% at 50% conversion and 46% at 99% conversion. It can be assumed that due to the inclusion complex formation for the alkyl moiety of the ester, the latter was the first subjected to hydrolysis with the formation of LA, which subsequently was converted into γ-VL.

Figure 17 shows the activities of the Ru@β-CD-Glycd catalyst in the hydrogenation of all tested substrates calculated taking into account the amount of absorbed hydrogen. Two opposite tendencies can be distinguished, which are characteristic of non-polar and polar substrates. The non-polar substrates

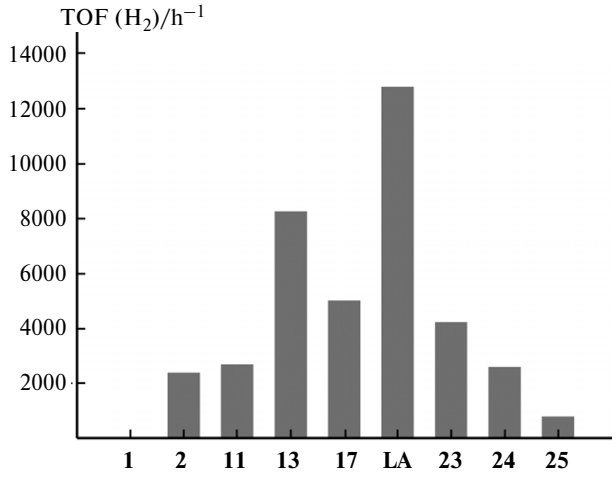

Fig. 17. Activity of the Ru@β-CD-Glycd catalyst in the hydrogenation of aromatic and unsaturated compounds, phenols, levulinic acid and its esters in an aqueous medium. Reaction conditions: 95 °C, 30 atm of H_2, V(substrate) = $V(H_2O)$.

represented by aromatic and unsaturated compounds such as benzene, biphenyl, and *trans*-stilbene readily form inclusion complexes with β-CD moieties of the carrier.[20,58] An increase in the substrate size leads to an increase in the catalyst activity in the order: benzene << biphenyl ≤ *trans*-stilbene (see Fig. 17). Herein, the presence of the CD moieties in the polymer stabilizing the ruthenium particles ensures the selective hydrogenation of the only one aromatic fragment of the substrate molecule located outside the CD hydrophobic cavity. Cyclodextrin itself acts as a protective group for the corresponding fragment of the substrate.[13,20]

Polar substrates, such as LA, phenol, methyl levulinate, on the contrary, tend to form hydrogen bonds with hydroxy groups of β-CD moieties and glycidyl chains and, as a result, form low stable inclusion complexes with the cyclodextrin cavity. As a result, it is possible to achieve high activities at low catalyst loading as compared to other ruthenium-containing systems.[30,57] An increase in the ability to form host—guest complexes between the substrate and the cyclodextrin moiety *via* non-polar substituent (ethyl and butyl levulinates, 4-*tert*-butylphenol) leads to a decrease in the system activity in hydrogenation, apparently, due to a less favorable orientation of the substrate in the complex (see Fig. 17).

Catalyst recycling. The possibility of a Ru@β-CD-Glycd catalyst reuse was studied in the hydrogenation of ethyl levulinate (**24**) as an example under two-phase conditions. The experiments were carried out according to the standard hydrogenation procedure in the presence of the Ru@β-CD-Glycd catalyst. After each reaction cycle, the catalyst was separated by precipitation with acetone, a "poor" solvent for cyclodextrin-based compounds,[23,59,60] dried, and reused. Seven cycles were carried out in total (Fig. 18). The total reaction turnover number (TON) reached 8770.

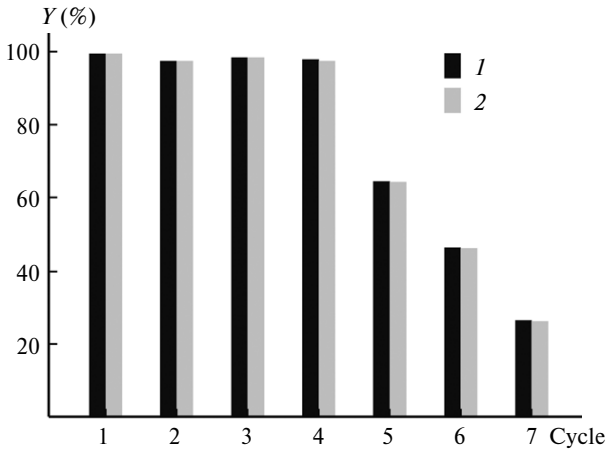

Fig. 18. The Ru@β-CD-Glycd catalyst recycling in the hydrogenation of ethyl levulinate *Y*(%): *1*, conversion, *2*, γ-VL yield; reaction conditions: 380 μL of ethyl levulinate, catalyst loading in the first cycle is 5 mg (substrate/Ru ≈ 1655 in the 1st cycle), 380 μL of H_2O, 30 atm of H_2, 95 °C, 1 h.

The catalyst was additionally dried in air before each reaction cycle to avoid a rapid downfall in its activity due to the accumulation of acetone and its adsorption on the surface of Ru NPs.[37] It can be seen that the quantitative conversion of substrate **24** and the yield of γ-VL were maintained during the first four cycles, the turnover number of which was 6505. The reaction is known to be highly sensitive to the ratio substrate/Ru,[57] therefore, the loss of the catalyst portion in each reaction cycle led to a decrease in the product yield. Nonetheless, the selectivity for γ-VL remained at the level of 99—100%.

In conclusion, we synthesized for the first time a water-soluble Ru@β-CD-Glycd catalyst based on Ru NPs stabilized with β-CD cross-linked with epichlorohydrin. For the hydrogenation of aromatic and unsaturated compounds, phenols, levulinic acid and its esters in an aqueous medium, it was found that the catalyst activity considerably depended on the polarity and size of the substrate. It was found out that the size of the substrate non-polar fragment determined its liability to form the inclusion complexes with β-CD moieties of the carrier. Hence, for compounds containing two aromatic fragments, the formation of the host—guest complex led to the hydrogenation of only the part of the substrate that was outside the cyclodextrin cavity.

As for the hydrogenation of phenols, LA and its esters, a downfall in the catalyst activity, on the contrary, accompanied an increase in the substrate tendency to form stronger inclusion complexes with β-CD moieties of the polymer due to the alkyl groups of the substituted phenol or levulinic ester. It was shown that the Ru@β-CD-Glycd catalyst can be slightly reused without any loss of activity and selectivity with additional drying from the solvent.

The authors are grateful to R. S. Borisov (A. V. Topchiev Institute of Petrochemical Synthesis of the Russian Academy of Sciences (TIPS RAS)) for assistance in carrying out mass spectrometry, M. A. Topchii (TIPS RAS) for performing NMR analysis,

A. A. Gud and A. A. Tereshchenko (National Research Center "Kurchatov Institute", Moscow) for carrying out analysis by small-angle X-ray scattering.

The work was financially supported by the Ministry of Science and Higher Education of the Russian Federation (Agreement No. 075-15-2021-1363).

No human or animal subjects were used in this research.

The authors declare no competing interests.

References

1. M. V. Polynski, V. P. Ananikov, *ACS Catal.*, 2019, **9**, 3991; DOI: 10.1021/acscatal.9b00207.
2. I. I. Protsenko, L. Zh. Nikoshvili, V. G. Matveeva, E. M. Sulman, *Top. Catal.*, 2020, **63**, 243; DOI: 10.1007/s11244-020-01223-0.
3. S. I. Serdyukov, M. I. Kniazeva, I. A. Sizova, Y. V. Zubavichus, P. V. Dorovatovskii, A. L. Maximov, *Mol. Catal.* 2021, **502**, 111357; DOI: 10.1016/j.mcat.2020.111357.
4. M. A. Golubeva, A. L. Maximov, *Appl. Catal. A: Gen.*, 2020, **680**, 117890; DOI: 10.1016/j.apcata.2020.117890.
5. D. Makeeva, L. Kulikov, A. Zolotukhina, A. Maximov, E. Karakhanov, *Mol. Catal.*, 2022, **517**, 112012; DOI: 10.1016/j.mcat.2021.112012.
6. V. Vinokurov, A. Glotov, Ya. Chudakov, A. Stavitskaya, E. Ivanov, P. Gushchin, A. Zolotukhina, A. Maximov, E. Karakhanov, Y. Lvov, *Ind. Eng. Chem. Res.*, 2017, **56**, 14043; DOI: 10.1021/acs.iecr.7b03282.
7. A. Yu. Stakheev, P. V. Markov, A. S. Taranenko, G. O. Bragina, G. N. Baeva, O. P. Tkachenko, I. S. Mashkovskii, A.S. Kashin, *Kinet. Catal.*, 2015, **56**, 733; DOI: 10.1134/S0023158415060130.
8. Yu. Liang, *Nanoscale Adv*. 2021, **3**, 6827; DOI: 10.1039/d1na00488c.
9. I. K. Goncharova, R. A. Novikov, I. P. Beletskaya, A. V. Arzumanyan, *J. Catal.*, 2023, **418**, 70; DOI: 10.1016/j.jcat.2023.01.004.
10. D. N. Gorbunov, M. V. Nenasheva, M. V. Terenina, Yu. S. Kardasheva, E. R. Naranov, A. L. Bugaev, A. V. Soldatov, A. L. Maximov, S. Tilloy, E. Monflier, E. A. Karakhanov, *Appl. Catal. A: Gen.*, 2022, **647**, 118891; DOI: 10.1016/j.apcata.2022.118891.
11. G. I. Dzhardimalieva, A. K. Zharmagambetova, S. E. Kudaibergenov, I. E. Uflyand, *Kinet. Catal.*, 2020, **61**, 198; DOI: 10.1134/S0023158420020044.
12. E. Karakhanov, A. Maximov, A. Zolotukhina, *Polymers*, 2022, **14**, 981; DOI: 10.3390/polym14050981.
13. I. S. Antipin, M. V. Alfimov, V. V. Arslanov, V. A. Burilov, S. Z. Vatsadze, Y. Z. Voloshin, K. P. Volcho, V. V. Gorbatchuk, Yu. G. Gorbunova, S. P. Gromov, S. V. Dudkin, S. Yu. Zaitsev, L. Ya. Zakharova, M. A. Ziganshin, A. V. Zolotukhina, M. A. Kalinina, E. A. Karakhanov, R. R. Kashapov, O. I. Koifman, A. I. Konovalov, V. S. Korenev, A. L. Maksimov, N. Zh. Mamardashvili, G. M. Mamardashvili, A. G. Martynov, A. R. Mustafina, R. I. Nugmanov, A. S. Ovsyannikov, P. L. Padnya, A. S. Potapov, S. L. Selektor, M. N. Sokolov, S. E. Solovieva, I. I. Stoikov, P. A. Stuzhin, E. V. Suslov, E. N. Ushakov, V. P. Fedin, S. V. Fedorenko, O. A. Fedorova, Yu. V. Fedorov, S. N. Chvalun, A. Yu. Tsivadze, S. N. Shtykov, D. N. Shurpik, M. A. Shcherbina, L. S. Yakimova, *Russ. Chem. Rev.*, 2021, **90**, 895; DOI: 10.1070/RCR5011.
14. S. Z. Vatsadze, A. L. Maximov, V. I. Bukhtiyarov, *Dokl. Chem.*, 2022, **502**, 1; DOI: 10.1134/S0012500822010013.
15. J. Lee, S.-S. Lee, S. Lee, H.B. Oh, *Molecules*, 2020, **25**, 4048; DOI: 10.3390/molecules25184048.
16. E. A. Karakhanov, A. L. Maksimov, E. A. Runova, *Russ. Chem. Rev.*, 2005, **74**, 97; DOI: 10.1070/RC2005v074n01ABEH000819.
17. F. Hapiot, E. Monflier, *Catalysts*, 2017, **7**, 173; DOI: 10.3390/catal7060173.
18. M. V. Papezhuk, V. A. Volynkin, V. T. Panyushkin, *Russ. Chem. Bull.*, 2022, **71**, 430; DOI: 10.1007/s11172-022-3430-5.
19. A. Nowicki, Y. Zhang, B. Léger, J.-P. Rolland, H. Bricout, E. Monflierc, A. Roucoux, *Chem. Commun.*, 2006, 296; DOI: 10.1039/b512838b.
20. S. Noël, B. Léger, R. Herbois, A. Ponchel, S. Tilloy, G. Wenz, E. Monflier, *Dalton Trans.*, 2012, **41**, 13359; DOI: 10.1039/c2dt31596c.
21. S. Kuklin, A. Maximov, A. Zolotukhina, E. Karakhanov, *Catal. Commun.*, 2016, **73**, 63; DOI: 10.1016/j.catcom.2015.10.005.
22. M. Chen, Q. Dong, W. Ni, X. Zhao, Q. Gu, G. Tang, D. Li, W. Ma, Zh. Hou, *ChemistrySelect* 2017, **2**, 10537; DOI: 10.1002/slct.201702229.
23. E. Renard, A. Deratani, G. Volet, B. Sebille, *Eur. Polym. J.*, 1997, **33**, 4957; DOI: 10.1016/S0014-3057(96)00123-1.
24. G. Crini, *Environ. Chem. Lett.*, 2021, **19**, 2383; DOI: 10.1007/s10311-021-01204-z.
25. A. T. N. Doan, V. T. H. Doan, J. Katsuki, Sh. Fujii, H. Kono, K. Sakurai, *ACS Omega*, 2022, **7**, 10890; DOI: 10.1021/acsomega.1c06194.
26. H. Becker, W. Berger, G. Domschke, E. Fanghenel, J. Faust, M. Fischer, F. Gentz, K. Gewald, R. Gluch, R. Mayer, K. Meller, D. Pavel, H. Schmidt, K. Schollberg, K. Schwetlick, E. Seiler, G. Zeppenfeld, *Organisch-Chemisches Grundpraktikum. Band II*, VEB Deutscher Verlag der Wissenschaften, Berlin, 1976.
27. G. S. Peters, O. A. Zakharchenko, P. V. Konarev, Y. V. Karmazikov, M. A. Smirnov, A. V. Zabelin, E. H. Mukhamedzhanov, A. A. Veligzhanin, A. E. Blagov, M. V. Kovalchuk, *Nucl. Instrum. Methods Phys. Res.*,

Sect. A, 2019, **945**, 162616; DOI: 10.1016/j.nima.2019.162616.
28. A. P. Hammersley, S. O. Svensson, M. Hanfland, A. N. Fitch, D. Häusermann, *High Pres. Res.*, 1996, **14**, 235; DOI: 10.1080/08957959608201408.
29. P. V. Konarev, V. V. Volkov, A. V. Sokolova, M. H. J. Koch, D. I. Svergun, *J. Appl. Cryst.*, 2003, **36**, 1277; DOI: 10.1107/S0021889803012779.
30. A. Maximov, A. Zolotukhina, V. Murzin, E. Karakhanov, E. Rosenberg, *ChemCatChem*, 2015, **7**, 1197; DOI: 10.1002/cctc.201403054.
31. J. Defaye, N. Evrard, S. Crouzy, H. Law, Pat. US 6.570.009 B1, May 27, 2003.
32. E. Renard, G. Volet, C. Amiel, *Polym. Int.*, 2005, **54**, 594—599; DOI: 10.1002/pi.1742.
33. X. Ao, J. A. Stenken, *Analyst*, 2003, **128**, 1143—1149; DOI: 10.1039/B308057A.
34. S. Rio, G. Peru, B. Léger, F. Kerdi, M. Besson, C. Pinel, E. Monflier, A. Ponchel, *J. Catal.*, 2020, **383**, 343; DOI: 10.1016/j.jcat.2019.10.021.
35. E. Norkus, *J. Incl. Phenom. Macrocycl. Chem.*, 2009, **65**, 237; DOI: 10.1007/s10847-009-9586-x.
36. D. Prochowicz, A. Kornowicz, I. Justyniak, J. Lewínski, *Coord. Chem. Rev.*, 2016, **306**, 331; DOI: 10.1016/j.ccr.2015.07.016.
37. E. Karakhanov, A. Maximov, A. Zolotukhina, Yu. Kardasheva, M. Talanova, *J. Inorg. Organomet. Polym. Mater.*, 2016, **26**, 1264; DOI: 10.1007/s10904-016-0399-2.
38. J. Y. Shen, A. Adnot, S. Kaliaguine, *Appl. Surf. Sci.*, 1991, **51**, 47; DOI: 10.1016/0169-4332(91)90061-N.
39. B. Folkesson, *Acta Chem. Scand.*, 1973, **27**, 287; DOI: 10.3891/acta.chem.scand.27-0287.
40. K. S. Kim, N. Winograd, *J. Catal.*, 1974, **35**, 66; DOI: 10.1016/0021-9517(74)90184-5.
41. B. E. Koel, G. Praline, H. I. Lee, J. M. White, *J. Electron Spectrosc. Relat. Phenom.*, 1980, **21**, 31; DOI: 10.1016/0368-2048(80)85035-3.
42. G. Beamson, D. Briggs, *High Resolution XPS of Organic Polymers: the Scienta ESCA300 Database*, Wiley, Chichester, 1992.
43. D. Briggs, G. Beamson, *Anal. Chem.*, 1992, **64**, 1729; DOI: 10.1021/ac00039a018.
44. M. Devillers, O. Dupuis, A. Janosi, J. P. Soumillion, *Appl. Surf. Sci.*, 1994, **81**, 83; DOI: 10.1016/0169-4332(94)90088-4.
45. B. Gidwani, A. Vyas, *Colloids Surfaces B: Biointerfaces*, 2014, **114**, 130; DOI: 10.1016/j.colsurfb.2013.09.035.
46. H. Rachmawati, C. A. Edityaningrum, R. Mauludin, *AAPS Pharm. Sci. Tech.*, 2013, **14**, 1303; DOI: 10.1208/s12249-013-0023-5.
47. E. A. Karakhanov, A. L. Maksimov, A. V. Zolotukhina, S. V. Kardashev, *Petrol. Chem.*, 2010, **50**, 290; DOI: 10.1134/S0965544110040067.
48. E. A. Karakhanov, A. L. Maximova, A. V. Zolotukhina, M. V. Terenina, A. V. Vutolkina, *Petrol. Chem.*, 2016, **56**, 491; DOI: 10.1134/S0965544116060037.
49. N. Szaniszlo, E. Fenyvesi, J. Balla, *J. Incl. Phenom. Macrocycl. Chem.*, 2005, **53**, 241; DOI: 10.1007/s10847-005-0245-6.
50. Sh. Nishimura, *Handbook of Heterogeneous Catalytic Hydrogenation for Organic Synthesis*, Wiley, New York, 2001.
51. T. Maegawa, A. Akashi, K. Yaguchi, Yo. Iwasaki, M. Shigetsura, Ya. Monguchi, H. Sajiki, *Chem.—Eur. J.*, 2009, **15**, 6953; DOI: 10.1002/chem.200900361.
52. R. L. Augustine, *Heterogeneous Catalysis the Synthetic Chemist*, Marcel Dekker, Inc., New York, 1995.
53. J. Shen, X. Yin, D. Karpuzov, N. Semagina, *Catal. Sci. Technol.*, 2013, **3**, 208; DOI: 10.1039/C2CY20443F.
54. A. Kalantar, H. Backman, J. H. Carucci, T. Salmi, D. Yu. Murzin, *J. Catal.*, 2004, **227**, 60; DOI: 10.1016/j.jcat.2004.06.027.
55. L. E. Hunt, S. A. Bourne, M. R. Caira, *Biomolecules*, 2021, **11**, 45; DOI: 10.3390/biom11010045.
56. B. V. K. J. Schmidt, M. Hetzer, H. Ritter, C. Barner-Kowollik, *Macromolecules*, 2011, **44**, 7220; DOI: 10.1021/ma2011969.
57. A. L. Maximov, A. V. Zolotukhina, A. A. Mamedli, L. A. Kulikov, E. A. Karakhanov, *ChemCatChem*, 2018, **10**, 222; DOI: 10.1002/cctc.201700691.
58. H. Bricout, L. Caron, D. Bormann, E. Monflier, *Catal. Today*, 2001, **66**, 355; DOI: 10.1016/S0920-5861(00)00631-3.
59. Y. Liu, C.-C. You, S. He, G.-S. Chen, Y.-L. Zhao, *J. Chem. Soc. Perkin Trans.*, 2002, **2**, 463; DOI: 10.1039/B110159E.
60. J. R. Jiménez Blanco, J. M. García Fernández, A. Gadelle, J. Defaye, *J. Carbohydr. Res.*, 1997, **303**, 367; DOI: 10.1016/S0008-6215(97)00176-6.

Received December 9, 2022;
in revised form February 1, 2023;
accepted February 7, 2023